Zwitterionic Rhodium and Iridium Complexes based on a Carboxylate Bridge-Functionalized Bis-N-Heterocyclic Carbene Ligand: Synthesis, Structure, Dynamic Behavior and Reactivity

Raquel Puerta-Oteo,[†] M. Victoria Jiménez,[†,*] Fernando J. Lahoz,[†] Francisco J. Modrego,[†] Vincenzo Passarelli[§,†] and Jesús J. Pérez-Torrente[†,*]

[†] Departamento de Química Inorgánica, Instituto de Síntesis Química y Catálisis Homogénea–ISQCH, Universidad de Zaragoza–CSIC, Facultad de Ciencias, C/ Pedro Cerbuna, 12, 50009 Zaragoza, Spain

[§] Centro Universitario de la Defensa, Ctra. Huesca s/n, ES–50090 Zaragoza, Spain

ABSTRACT: A series of water-soluble zwitterionic complexes featuring a carboxylate bridge-functionalized bis-N-heterocyclic carbene ligand of formula $[Cp*M^{III}Cl\{(MeIm)_2CHCOO\}]$ and $[M^{I}(diene)\{(MeIm)_2CHCOO\}]$ (M = Rh, Ir; diene = cod, nbd) have been prepared from the salt 1,1-bis(*N*-methylimidazolium)acetate bromide and suitable metal precursor. The solid state structure of both types of complexes shows a boat-shaped 6-membered metallacycle derived of the $\kappa^2 C,C'$ coordination mode of the bis-NHC ligand. The uncoordinated carboxylate fragment is found at the *bowsprit* position in the $Cp*M^{III}$ complexes whereas in the $M^{I}(diene)$ complexes is at the *flagpole* position of the metallacycle. The complexes $[Rh^{I}(diene)\{(MeIm)_2CHCOO\}]$ (diene = cod, nbd) exist as two conformational isomers in dichloromethane, *bowsprit* and *flagpole*, that interconvert through the boat-to-boat inversion of the metallacycle. An inversion barrier of around 17 kcal·mol^{-1} has been determined by 2D EXSY NMR measurements for $[Rh^{I}(cod)\{(MeIm)_2CHCOO\}]$. Reaction of zwitterionic $Cp*M^{III}$ complexes with methyl triflate or tetrafluoroboric acid affords the cationic complexes $[Cp*M^{III}Cl\{(MeIm)_2CHCOOMe\}]^+$ or $[Cp*M^{III}Cl\{(MeIm)_2CHCOOH\}]^+$ (M = Rh, Ir) featuring carboxy- and methoxycarbonyl functionalized methylene-bridged bis-NHC ligands, respectively. Similarly, complexes $[M^{I}(diene)\{(MeIm)_2CHCOOMe\}]^+$ (M = Rh, Ir) have been prepared by alkylation of the corresponding zwitterionic $M^{I}(diene)$ complexes with methyl triflate. In contrast, reaction of $[Ir^{I}(cod)\{(MeIm)_2CHCOO\}]$ with HBF$_4$·Et$_2$O, CH$_3$OTf, CH$_3$I or I$_2$, gives cationic iridium(III) octahedral complexes $[Ir^{III}X(cod)\{(MeIm)_2CHCOO\}]^+$ (X = H, Me or I) featuring a tripodal coordination mode of the functionalized bis-NHC ligand. The switch from $\kappa^2 C,C'$ to $\kappa^3 C,C',O$ coordination of the bis-NHC ligand accompanying the oxidative addition prevents the coordination of the anions eventually formed in the process that remain as counterions.

INTRODUCTION

N-Heterocyclic carbenes (NHCs) have become a powerful tool in modern chemistry. Topological and electronical versatility together with their remarkable strong σ-donor and weak π-acceptor features, and the relative easy synthesis of suitable precursors make them attractive key ligands for the design of coordination/organometallic complexes for a broad range of applications such as catalysis, medicinal chemistry and materials science.[1,2,3]

Multidentate/poly-NHC ligands provide privileged access to polynuclear, high oxidation state or mixed valence complexes with a tunable coordination sphere. Largely, these ligands obligate to a determined coordination geometry that results in complexes with interesting physical properties and chemical reactivity. The chelate or pincer effects derived from coordination of multidentate NHC ligands results in the formation of stable metal-ligand platforms with easily modulable properties that offer an extra stabilization which allows the identification of key intermediates in small molecule activation or the opening of new reaction pathways in both stoichiometric or catalytic reactions.[4,5] In addition, a potential hemilabile character can be anticipated in some cases through functionalization either on the wingtip or in the skeleton of the multidentate NHC ligands. In this context, wingtip functionalization of NHCs has been recently widely explored by several research groups, either to modulate their electronic and steric properties or to immobilize the NHC metal complexes on insoluble supports.[6,7]

Although symmetrical poly-NHCs, mainly tris- and tetra-NHCs, provided complexes with a facial array of the carbene donors in the case of tris(imidazolydene)borates[8] or a variety of metallosupramolecular assemblies,[9] the bis-NHCs are by far the most extensively studied ligands in both coordination and organometallic chemistry (Chart 1).[10] The two NHC fragments can be bonded with an aliphatic linker of variable length (**A**) and mononuclear chelate or dinuclear complexes can be formed depending on the length and rigidity of the linker or the sterical requirements of the wingtips.[11,12] The linker between the two NHC edges can have a P, O, S, or N-donor functional group rendering a potential tridentate coordination and providing pincer (**B**)[13,14] or tripodal (**C**)[15,16] bis-NHC type ligands. In contrast, the linearly opposed

arrangement of the two carbene units in benzobis(imidazolylidene) ligands (**D**) results in dinuclear complexes that have found application in several catalytic processes.[17] On the other hand, ditopic triazolylidenes (**E**)[18] and anionic NHCs which bear remote anionic group (**F**)[19] have drawn much less attention. Notably, the rigid structure of the latter prevents unwanted ion-pairing between the metal and the remote anionic moiety, and provides an easy access to the corresponding zwitterionic metal complexes that are generally water soluble and therefore particularly attractive in catalysis.[20, 21]
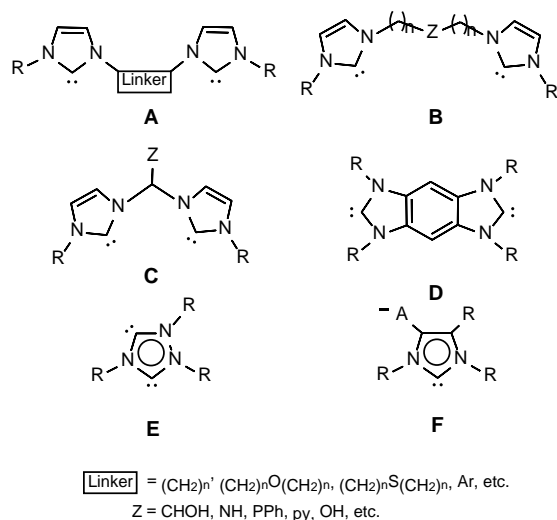

Chart 1. Selected functionalized bis-NHC ligands based on imidazole units and other ditopic NHCs.

Whereas there are many studies describing the pincer-like coordination, i.e. tridentate-*mer*, of functionalized bis-NHC ligands (**B**), the number of complexes having type **C** bis-NHC ligands is rather scarce. Chart 2 shows the functionalized methylene-bridge bis-NHC[16,22,23,24] or related bis-triazolyl ligands[25,26] so far reported. Hydroxymethyl-funtionalized methylene-bridged bis-imidazolium salts have been recently reported by Kühn and the corresponding copper, silver, gold and palladium complexes have been described.[27,28,29] However, in most of these complexes the bis-NHC ligands exhibit a $\kappa^2 C,C$ bidentate coordination mode with an uncoordinated functional group in the skeleton.[26-30] In fact, advantage of the presence of an hydroxyl group has been taken for the immobilization of palladium complexes on solid supports.[27,31] As far as we know, the only example of tripodal $\kappa^3 C,C,O$ coordination is a rhodium(III) compound having a bis-NHC ligand functionalized with a 2-phenolate substituent in the bridge.[16]

Inspired by this ligand scaffold and with the aim of developing our research on the synthesis and catalytic applications of transition-metal complexes containing functionalized NHC ligands with a hemilabile character,[32, 33,34,] we envisaged the potential of a carboxylate-functionalized methylene-bridged bis-NHC ligand for the construction of a versatile metal-ligand platform. The carboxylate group at the linker could confer hemilabile properties to the ligand while imparting water solubility to the complexes. In this respect, we have recently reported[35] the synthesis of the zwitterionic iridium(I) compound [Ir(cod){(MeIm)$_2$CHCOO}] which is a catalyst precursor for the hydrogenation of CO_2 to formate in water. Reactivity studies and mechanistic investigations support the dihydrido Ir(III) octahedral [IrH$_2$(H$_2$O){(MeIm)$_2$CHCOO}] complex as the catalytic active species.

We report herein on the synthesis and structure of zwitterionic rhodium and iridium complexes derived from the bis(*N*-methylimidazolium)acetate bromide salt. Reactivity studies have shown that the uncoordinated carboxylate moiety in the complexes is a reactive site and consequently complexes featuring carboxy- and methoxycarbonyl functionalized bis-NHC ligands have been prepared. In contrast, oxidation of the iridium center results in the formation of octahedral iridium(III) complexes enforcing a $\kappa^3 C,C',O$ coordination of the ligand.
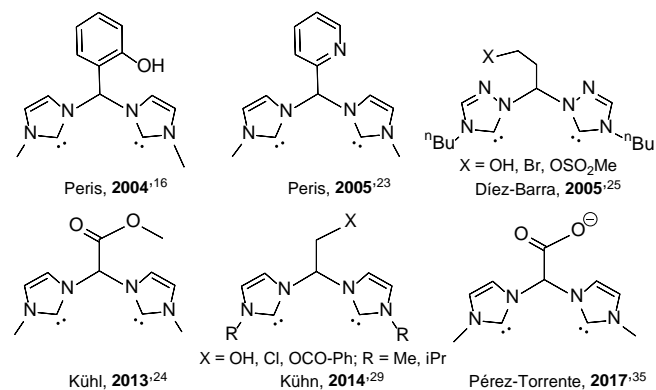

Chart 2. Functionalized methylene-bridged bis-NHC or related bis-triazolyl ligands (Type **C**).

RESULTS AND DISCUSSION

Synthesis and structure of the carboxylate-functionalized bis-imidazolium salt [(MeImH)$_2$CHCOO]Br. The salt 1,1'-bis(*N*-methylimidazole)-acetate bromide, precursor of the carboxylate-functionalized bis-NHC ligand, was prepared by reaction of ethyl dibromoacetate with an excess of *N*-methylimidazole in THF at 343 K and isolated as a white hygroscopic solid in 79% yield after recrystallization from methanol/acetone.[35] The zwitterionic compound [(MeImH)$_2$CHCOO]Br (**1**) likely is formed from the intermediate ester functionalized bis-imidazolium salt, [(MeImH)$_2$CHCOOEt]Br$_2$, by nucleophilic substitution by bromide under anhydrous reaction conditions. The salt was fully characterized by means of analytical and spectroscopic techniques. Furthermore, the zwitterionic character of **1** has been confirmed unambiguously by a single crystal X-ray diffraction study.

A view of **1·**3 H$_2$O is shown in Figure 1. Bond lengths and angles of the imidazolium fragment are similar to those of related methylene bridged bis-NHC derivatives.[27,36,37] In addition carbon–oxygen bond length [C(8)–O(1) 1.238(3) Å] is indicative of a charge delocalization within the carboxylate group.[38] Intermolecular C–H···O and C–H···Br contacts are discussed in the Supporting Information.
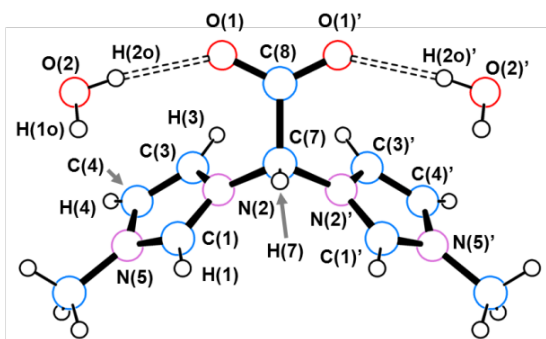
Figure 1. View of the bis-imidazolium cation [(MeImH)$_2$CHCOO]$^+$ in $1\cdot3$ H$_2$O. Selected bond lengths (Å) and angles (°) are C(1)-N(2) 1.326(4), C(1)-N(5) 1.320(5), C(3)-C(4) 1.349(5), C(3)-N(2) 1.384(5), C(4)-N(5) 1.386(6), C(8)-O(1) 1.238(4), O(1)-C(8)-O(1)' 127.7(5). Hydrogen bond parameters (Å, °): O(2)-H(2o) 0.83(6), O(2)···O(1) 2.923(7), H(2o)···O(1) 2.10(6), O(2)-H(2o)-O(1) 171(5). ´ symmetry operator +x, −y+1/2, +z

Synthesis of zwitterionic [Cp*M^{III}Cl{(MeIm)$_2$CHCOO}] (M = Rh, Ir) complexes. The generation of free NHC ligands from the corresponding imidazolium salts can be problematic for some NHC systems. Unfortunately, the attempts to isolate the free bis-NHC ligand by deprotonation of [(MeImH)$_2$CHCOO]Br (1) using NaH, K^{t}BuO or potassium bis(trimethylsilyl)amide (KHMDS) were unsuccessful. As an alternative, the *in situ* deprotonation of 1 at low temperature under different conditions followed by reaction with the acetonitrile solvates [Cp*M(NCCH$_3$)$_3$]$^{2+}$ (M = Rh, Ir) also gave poor results. Most probably, the acidity of the CH proton at the bridging position of the pro-ligand interferes in the deprotonation of the imidazolium fragments likely resulting in the degradation of the ligand. Therefore, the silver-NHC transmetallation strategy was used to prepare the complexes [Cp*M^{III}Cl{(MeIm)$_2$CHCOO}] (M = Rh, Ir).

Scheme 1. Synthesis of zwitterionic [(MeIm)$_2$CHCOOAg]$_2$ and [Cp*MCl{(MeIm)$_2$CHCOO}] (M = Rh, Ir) complexes.
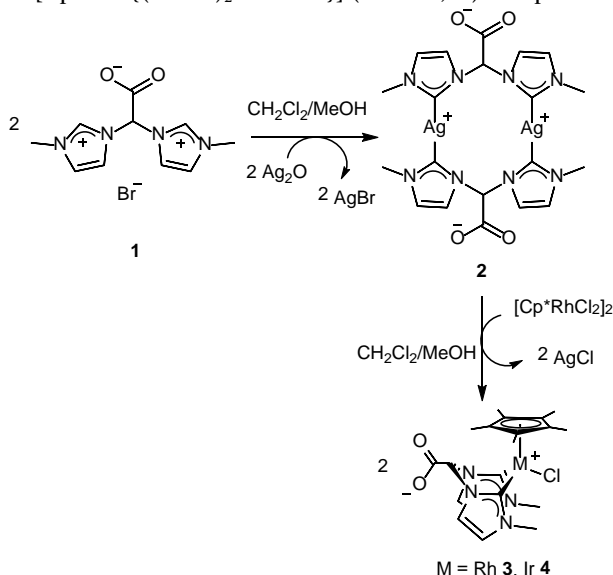
The preparation of the silver-NHC complex [(MeIm)$_2$CHCOOAg]$_2$ (2) was successfully achieved following a modified protocol of Youngs *et al.*[39] by reacting 1 with silver oxide in MeOH/CH$_2$Cl$_2$. The ESI+ mass spectrum of 2 showed

a peak at *m/z* 654.0 suggesting a dinuclear structure in which each Ag^I ion could be coordinated by two carbene moieties of two different bis-NHC ligands rendering a zwitterionic structure similar to that of related methylene-bridged bis-NHC silver complexes.[27,28,39,40,41] Also, the ^{1}H NMR spectrum of 2 showed two resonances for the N-Me groups and one -C*H*COO signal suggesting a nonsymmetric dinuclear framework with two equivalent bis-NHC ligands.[28] Unfortunately the low solubility of 2 in deuterated solvents prevented a reliable ^{13}C assignment and eventually a detailed structural elucidation of 2 in solution.[27,40]

Reaction of [(MeIm)$_2$CHCOOAg]$_2$ (2) with [Cp*MCl$_2$]$_2$ gave high yields of the compounds [Cp*RhCl{(MeIm)$_2$CHCOO}] (3) or [Cp*IrCl{(MeIm)$_2$CHCOO}] (4). Notably both compounds are highly soluble not only in chlorinated solvents, CH$_3$CN, MeOH or acetone but also in water.

The ^{1}H and ^{13}C{^{1}H} NMR data of 3 and 4 indicate a zwitterionic structure of C_s symmetry resulting from the κ^2C,C' coordination of the bis-NHC ligand with an uncoordinated carboxylate group that bears a delocalized negative charge. Indeed the imidazole-2-carbene protons showed two doublets in the range δ 7-8 ppm and two equivalent N-Me groups are observed (^{1}H, ^{13}C). Interestingly the methyne resonance is seen at δ 5.83 (3) and 5.72 ppm (4) suggesting that the ^{1}H chemical shift of the methyne moiety is extremely sensitive to the coordination mode of the bis-NHC ligand. In fact, this resonance was found downfield shifted up to δ 7.76 ppm in the silver dinuclear complex 2 in which a $1\kappa C,2\kappa C$ coordination mode was proposed. The zwitterionic complexes frequently crystallize with methanol (see below) which is observed in the corresponding NMR spectra. In particular, the ^{1}H NMR spectrum of 3 shows a doublet at δ 3.43 ppm (J_{H-H} = 4.9 Hz) which is assigned to a methyl group of a MeOH molecule likely hydrogen-bonded to the carboxylate group. The ^{13}C{^{1}H}-apt NMR spectrum of 3 in CDCl$_3$ shows a doublet at δ 168.0 ppm (J_{C-Rh} = 50.7 Hz) for the equivalent C$_{NCN}$ atoms which further confirms the coordination of the bis-NHC ligand to the rhodium centre. The carbon atoms of the CHCOO moiety, also sensitive to the coordination mode of the ligand, are observed at δ 163.3 and 74.6 ppm, respectively. Comparing 3 and 4 neither of the two resonances in ^{13}C{^{1}H} NMR spectra resulted significantly affected by the metal centre. However, the equivalent C$_{NCN}$ atoms were observed as sharp singlet around δ 151 ppm in the ^{13}C{^{1}H}-apt NMR spectrum of 4 in CD$_2$Cl$_2$, high-field shifted compared to 3.

The presence of an uncoordinated carboxylate group in complexes 3 and 4 makes possible the existence of up to four stereoisomers of C_S symmetry all compatible with the spectroscopic information. The chelate coordination of the bis-NHC ligand to the metal centre results in the formation of a 6-membered boat metallacycle in which both the carboxylate fragment and the remaining ligands at the metal centre can occupy two different positions, *flagpole* or *bowsprit*, according to the IUPAC.[42] Assuming that the rather bulky Cp* ligand is located at a *flagpole* position, the uncoordinated carboxylate moiety is directed either towards the Cp*M fragment (*flagpole* isomer) or away from it (*bowsprit* isomer), the latter configuration adapting to the steric hindrance exerted by the Cp*M fragment. (Figure 2). Indeed, DFT calculations have shown that the corresponding isomers having the Cp* ligand in *bowsprit* position are much less stable (see below). Interestingly, the existence of the *bowsprit* isomer in complexes 3 and 4 is confirmed in the ^{1}H-

[1]H-NOESY spectrum that showed a weak proximity cross peak between the methyne resonance and the methyl protons of the Cp* ring (see Supporting Information).
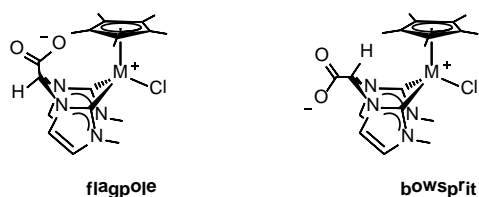

Figure 2. Stereoisomers for **3** and **4** featuring the carboxylate moiety in *flagpole* or *bowsprit* positions.

The ORTEP view of the solid state structures of **3**·CH$_3$OH and **4**·CH$_3$OH is shown in Figure 3 and selected bond lengths and angles are given in Table 1. In agreement with the solution NMR data for both **3** and **4**, the $\kappa^2 C,C'$ coordination of the bis-NHC ligand affords a 6-membered ring with a boat conformation in which the chlorido ligand and the carboxylate group occupy the bowsprit positions. The coordination sphere of the metal centre is completed by the η^5–pentamethylcyclopentadienyl ligand rendering a pseudo tetrahedral coordination polyhedron. Notably, the pitch (⩔) and yaw (⩗) angles[43] (see Supporting Information) of the imidazolyl ring are close to zero (⩔ 1.5°, **3**; 0.9°, **4**; ⩗ 2.1°, **3**; 2.7°, **4**) indicating a virtually ideal arrangement of each imidazolyl moiety with respect to the rhodium-NHC bond. As for the carboxylate group, as a clue of the charge delocalization within the COO group, similar carbon-oxygen bond lengths are observed (Table 1),[38] the slight difference being reasonably the result of the intermolecular hydrogen bond O(1)···H(3o)–O(3) to the lattice methanol molecule (Figure 3A and 3B, Table 1).

Table 1. Selected bond lengths (Å), interatomic distances (Å) and angles (°) in **3**·MeOH, **4**·MeOH, **8**, and **9**.

	3	4	8	9
M–C(1)	2.018(2)	2.017(4)	2.021(3)	2.037(3)
M–C(10)	-	-	2.033(2)	2.027(4)
M–Cl	2.4135(8)	2.4500(11)	2.4083(8)	-
M–O(3)	-	-	-	2.207(2)
M–ct	1.8489(3)	1.8508(2)	1.8451(2)	1.8338(4)
C(8)–O(1)	1.253(4)	1.253(7)	1.189(4)	1.202(4)
C(8)–O(2)	1.236(4)	1.230(7)	1.321(4)	1.326(5)
C(1)-M-C(1)′	85.26(12)	85.3(2)	-	-
C(1)-M-C(10)	-	-	83.95(11)	84.61(14)
O(1)-C(8)-O(2)	129.0(3)	129.6(5)	125.8(3)	126.5(4)
O(3)–H(3o)	0.81(3)	0.840(4)	-	-
H(3o)···O(1)	2.11(4)	2.078(4)	-	-
O(1)···O(3)	2.874(3)	2.860(5)	-	-
O(3)-H(3o)-O(1)	157(3)	154.73(3)	-	-

ct, centroid of C$_5$ ring of the η^5-pentamethylcyclopentadienyl ligand. ′ symmetry operator +x; ½–y; z.
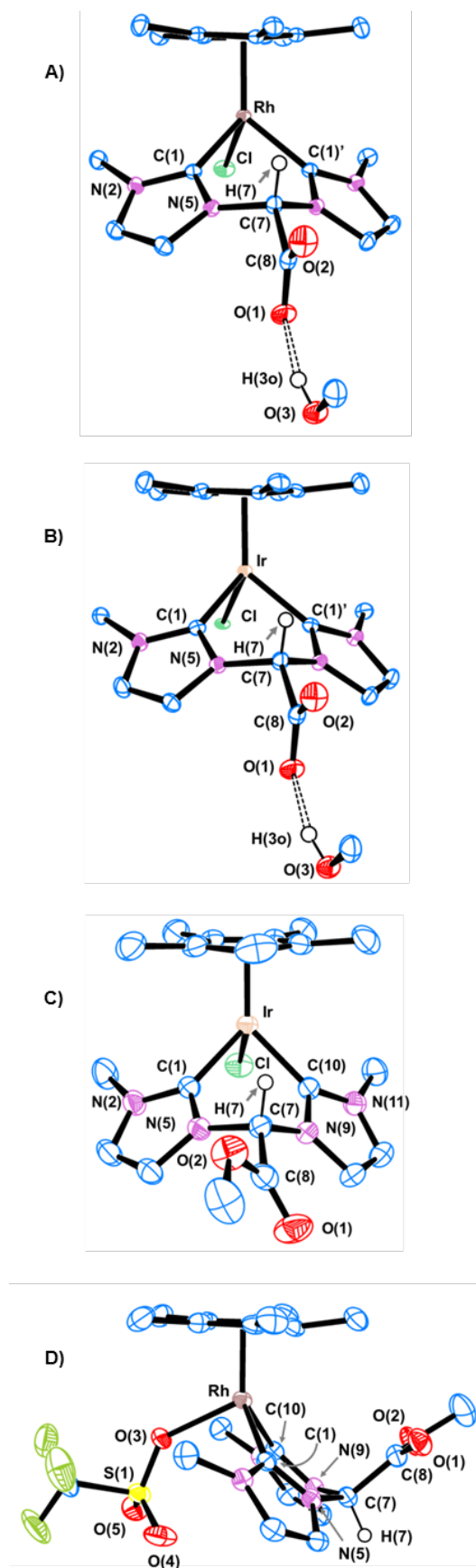

Figure 3. ORTEP view of **3**·CH$_3$OH (A), **4**·CH$_3$OH (B), and the cationic complex of **8** (C) and **9** (D). Ellipsoids are at the 50 % of probability and most hydrogen atoms are omitted for clarity.

Reactivity of zwitterionic [Cp*M^{III}Cl{(MeIm)₂CHCOO}] (M = Rh, Ir) complexes. The unusual features of these zwitterionic complexes prompted us to study their reactivity. On the one hand, the uncoordinated carboxylate fragment with an overall negative formal charge is a nucleophilic site and its reaction with electrophiles such as H⁺ or Me⁺ can be envisaged. On the other hand, the chlorido abstraction by reaction with silver salts should result in a coordinative vacancy that can be finally occupied by a solvent molecule, such as acetonitrile, a ligand present in the reaction medium, or even the uncoordinated carboxylate moiety.

The addition of HBF₄·Et₂O to a dichloromethane solution of the zwitterionic complexes **3** or **4** gave yellow-orange solutions of the corresponding cationic complexes [Cp*MCl{(MeIm)₂CHCOOH}]⁺ (M = Rh, **5**; Ir, **6**) bearing a carboxy group that results from the protonation of the carboxylate fragment of the parent complexes. In the same way, reaction of the zwitterionic complexes with methyl trifluoromethanesulfonate (MeOTf) afforded the corresponding cationic complexes [Cp*MCl{(MeIm)₂CHCOOMe}]⁺ (M = Rh, **7**; Ir, **8**) resulting from the alkylation of the carboxylate fragment (Scheme 2). The complexes were isolated as the tetrafluoroborate or triflate salts as air-stable crystalline yellow solids in 65-90% yields.

Scheme 2. Synthesis of cationic complexes [Cp*MCl{(MeIm)₂CHCOOE}]⁺ (E = H, Me; M = Rh, Ir).

M = Rh, **3**; Ir, **4**

E = H, X = BF₄; M = Rh, **5**; Ir, **6**
E = Me, X = OTf; M = Rh, **7**; Ir, **8**
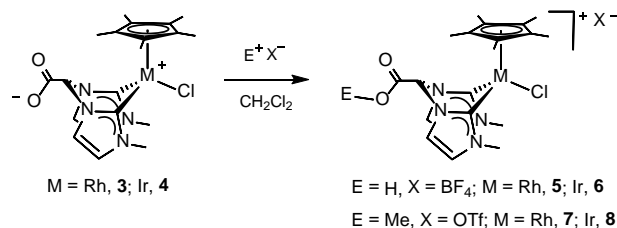
The cationic complexes have been fully characterized using standard spectroscopic techniques. Notably, the ATR-IR spectra of the complexes exhibited absorption bands around 1740-1760 cm⁻¹ corresponding to the carboxy and methoxycarbonyl groups, clearly shifted compared to the 1650 cm⁻¹ absorption band exhibited by the zwitterionic complexes confirming the change of the carboxylate environment (See Supporting Information). The NMR spectra of these compounds are very similar to those of the zwitterionic parent complexes except for the resonances of the new functional groups. The ¹H NMR spectra of **5** and **6** showed a broad resonance at δ 4.14 ppm assigned to the –OH of the carboxy group. The methyl group of the methoxycarbonyl fragment in complexes **7** and **8** was observed around δ 4.1 and 55 ppm in the ¹H and ¹³C{¹H} NMR spectra, respectively.

The crystal structure of **8** was determined in the solid state and the ORTEP view of the cationic complex [Cp*IrCl{(MeIm)₂CHCOOMe}]⁺ in **8** is shown in Figure 3C. Similarly to **3** and **4** the κ²C,C' coordination of the bis-NHC moiety renders a 6-membered ring with a boat conformation in which the ester group and the chlorine atom occupies bowsprit positions. The bite angle of the bis-NHC ligand [C(1)-Ir-C(10) 83.95(11)°] is similar to that observed in **3** [85.26(12)°] and **4** [85.3(2)°]. Nevertheless, although the two nonequivalent imidazolyl moieties exhibit similar yaw angles [C(1), ↗ 3.8; C(10), ↗ 4.2], different pitch (↘) angles are observed [C(1), ↘ 1.7; C(10), ↘ 5.8] reasonably in connection

with the almost coplanar arrangement of the COO moiety and the imidazolyl ring C(10)-N(11)-C(12)-C(13)-N(9) [O(1)-C(8)-C(7)-N(9) –19.60(42)°]. Finally it is worth a mention that the significantly different carbon–oxygen bond lengths observed for the ester group, namely C(8)–O(1) 1.189(4) Å and C(8)–O(2) 1.321(4) Å, nicely fit in with the presence of localized double and single carbon–oxygen bonds within the COO group.[38]

The abstraction of the chlorido ligand was explored on [Cp*RhCl{(MeIm)₂CHCOO}] (**3**) and [Cp*RhCl{(MeIm)₂CHCOOMe}]OTf (**7**). The reaction of **3** with either stoichiometric amounts or excess of a range of silver salts (AgX, X = BF₄, PF₆, SbF₆ or OTf) resulted in the precipitation of AgCl. However, the isolated solids obtained after removing the insoluble silver chloride showed broad ¹H resonances suggesting the formation of several species probably in a rapid exchange. Likely, interaction between the Ag⁺ ions and the uncoordinated carboxylate group results in the incomplete precipitation of AgCl and is responsible of the lack of selectivity of the reactions. Reaction of **3** with TlPF₆ gave similar results even when using coordinating solvents such as acetonitrile or acetone. On the other hand, the addition of AgOTf to a solution of **7** in dichloromethane gave good yields of [Cp*Rh(OTf){(MeIm)₂CHCOOMe}]OTf (**9**) (Scheme 3).

The ORTEP view of the cation [Cp*Rh(OTf){(MeIm)₂CHCOOMe}]⁺ in **9** is shown in Figure 3D. Similarly to **3**, **4** and **8**, the coordination polyhedron is pseudo tetrahedral with a κ²C,C' coordination of the bis-NHC ligand {C(1)–Rh–C(10) 84.61(14)°}. When compared with **8**, smaller deviations from an ideal arrangement of the imidazolyl moieties with respect to the rhodium-NHC bond are observed for **9** [C(1), ↘ 2.0, ↗ 2.5; C(10), ↘ 3.9; ↗ 1.0], reasonably as a consequence of the local symmetry at the C(7) carbon atom [O(1)-C(8)-C(7)-N(5) 27.6(5)°, O(2)-C(8)-C(7)-N(9) –30.1(4)°]. Notably, at variance with **8**, the COOMe group occupies a flagpole position of the six member ring Rh-C(1)-N(5)-C(7)-N(9)-C(10). Reasonbly as a result of the steric repulsion between the Cp* ligand and the COOMe group, the ring adopts a boat conformation flatter than that of **8**[44] exhibiting interplanar angles significantly smaller than in **8** (Table 2).
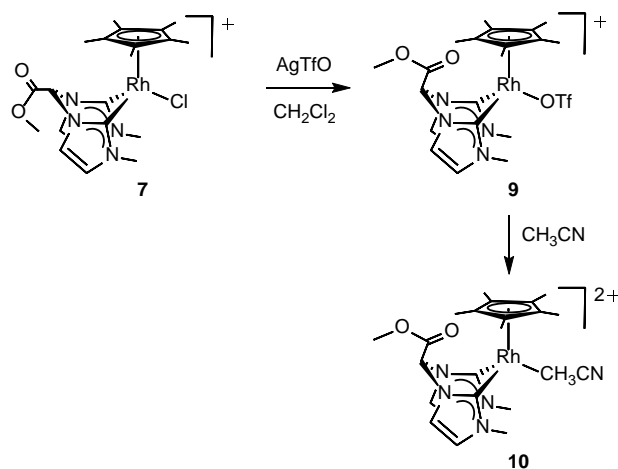
The ¹H and ¹³C{¹H} NMR spectra of **9** in CD₂Cl₂ are very similar to those of the parent complex **7** indicating the κ²C,C' coordination of the bis-NHC moiety. In addition, the two observed ¹⁹F resonances (δ -78.83 and -78.91 ppm) confirm the presence of two different triflate groups, one coordinated and the other acting as the counterion.

The triflate ligand in **9** is labile and was easily replaced by acetonitrile affording [Cp*Rh(NCCH₃){(MeIm)₂CHCOOMe}] (OTf)₂ (**10**) by reaction of **9** with neat acetonitrile (Scheme 3). Confirming the presence of coordinated acetonitrile, ¹H NMR spectrum showed a singlet at δ 2.52 ppm for its methyl group and the ¹³C{¹H}-apt spectrum exhibited two resonances at δ 127.7 and 4.65 ppm corresponding to the quaternary and methyl carbons of coordinated CH₃CN, respectively.

The molar conductivities of complexes **7**, **9** and **10** were measured in nitromethane. The molar conductivity for complex **7** is in accordance with a 1:1 electrolyte (85.1 Ω⁻¹·cm²·mol⁻¹). However, complexes **9** and **10** gave values corresponding to 2:1 electrolytes, 166.4 and 166.1 Ω⁻¹·cm²·mol⁻¹, respectively, which evidences the lability of the triflate ligand in **9**.

Scheme 3. Reactivity of complex [Cp*RhCl{(MeIm)$_2$CHCOOMe}]OTf (**7**).

Table 3. Calculated Gibbs free energy differences $\Delta G = G_{bowsprit} - G_{flagpole}$ for [Cp*MCl(L)], [Cp*MX(LMe)]$^+$ (X = Cl, OTf) and [Cp*M(NCCH$_3$)(LMe)]$^{2+}$ (M = Rh, Ir), L = (MeIm)$_2$CHCOO in methanol, dichloromethane and gas phase.

	ΔG (kcal·mol^{-1})		
	MeOH	CH$_2$Cl$_2$	Gas phase
[Cp*RhClL] (**3**)	2.44	3.08	5.54
[Cp*IrClL] (**4**)	3.93	3.19	5.98
[Cp*RhCl(LMe)]$^+$ (**7**)	5.05	6.06	2.87
[Cp*IrCl(LMe)]$^+$ (**8**)	4.52	3.71	2.70
[Cp*Rh(OTf)(LMe)]$^+$ (**9**)	2.11	2.92	4.14
[Cp*Ir(OTf)(LMe)]$^+$(**9-Ir**)	3.99	3.85	3.81
[Cp*Rh(NCCH$_3$)(LMe)]$^{2+}$ (**10**)	4.41	3.59	2.70
[Cp*Ir(NCCH$_3$)(LMe)]$^{2+}$ (**10-Ir**)	6.62	5.11	2.06

Table 2. Interplanar angles (°) for the six member metalacycle M-C(1)-N(5)-C(7)-N(5)-C(10) in **8**, **9**, **11**, **12**, and **14**.

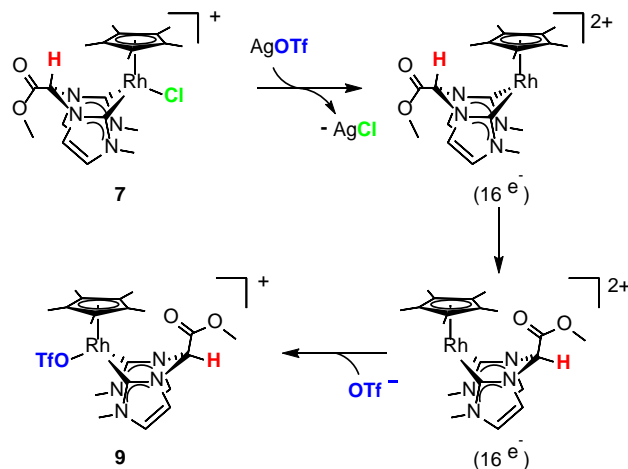| Compound	M	α	β
8	Ir	50.4	29.1
9	Rh	35.5	21.0
11	Rh	41.3	37.1
12	Rh	42.5	33.2
14	Ir	46.1	39.7

According to the experimental data we assume that, analogously to the iridium complex **8**, the carboxylate moiety in complex **7** occupies a *bowsprit* position. Thus, the formation of **9** involves a conformational change in the metallacycle that results in a change in the methoxycarbonyl position from *bowsprit* to *flagpole*. Likely, the reaction proceeds through the 16 electron intermediate species [Cp*Rh{(MeIm)$_2$CHCOOMe}]$^{2+}$ that undergoes a boat-to-boat inversion of the 6-membered metallacycle followed by the coordination of the triflate ion (Scheme 4).

The stereochemical change observed in the synthesis of **9** prompted us to carry out DFT calculations in order to determine the stability of the stereoisomers of the Cp*M^{III} complexes. First, the relative stability of the four stereoisomers of compound [Cp*RhCl{(MeIm)$_2$CHCOOMe}]$^+$ (**7**) has been studied. As expected, the isomers having the Cp* ligand in *bowsprit* position are much less stable than the corresponding *flagpole* isomers by 22-26 kcal·mol^{-1} (see Supporting Information). Thus, the structures of the *flagpole* and *bowsprit* isomers (Figure 2) have been optimized in methanol, dichloromethane and vacuum. Table 3 summarizes the calculated data representing ΔG (kcal·mol^{-1}) as the energy difference between the *bowsprit* and the *flagpole* isomers. On the steric grounds, the *flagpole* isomer is expected to be less stable as the substituent at the bridge of the bis-NHC ligands is directed towards the bulky pentamethylcyclopentadienyl ligand. Surprisingly, DFT calculations revealed that the *flagpole* isomer is more stable for all the Cp*M^{III} complexes including the yet unprepared **9-Ir** and **10-Ir** compounds, both in gas phase and in solution.

Scheme 4. Proposed mechanism for the stereochemical change observed in the synthesis of **9**.


The isolation of the less stable *bowsprit* isomer in the synthesis of complexes **3** and **4** should be related with the mechanism of formation. Both complexes result from the reaction of two dinuclear complexes, [Cp*MCl$_2$]$_2$ and [(MeIm)$_2$CHCOOAg]$_2$, reasonably through a multistep process involving the sequential transfer of both NHC fragments to the rhodium centre. It could be conceivable that the stereochemistry of some of the intermediate species determines the location of the carboxylate fragment in *bowsprit* position in the final product, which is compatible with the small energy difference between both stereoisomers. On the other hand, the alkylation of the carboxylate moiety in both complexes result in the clean formation of the cationic complexes **7** and **8** with retention of the stereochemistry. In contrast, the synthesis of **9** proceeds through an unsaturated intermediate species that allows the boat-to-boat inversion of the 6-membered metallacycle shifting the methoxycarbonyl group from the *bowsprit* to the *flagpole* position. Finally, the replacement of the triflate ligand for acetonitrile in **9** results in compound **10** for which the *flagpole* isomer is also more stable.

Synthesis of zwitterionic [M^I(diene){(MeIm)$_2$CHCOO}] (M = Rh, Ir; diene = cod, nbd) complexes. The synthesis of zwitterionic M^I(diene) (M = Rh, Ir) complexes was accomplished by the deprotonation *in situ* of the

functionalized bis-imidazolium salt. Due to the limited solubility of [(MeImH)$_2$CHCOO]Br (**1**), the selection of both solvent and base was crucial for the successful synthesis of this series of organometallic complexes. A preliminary study on the optimal reaction conditions using NaH as base evidenced that the presence of methanol is essential. The addition of NaH to a yellow suspension of **1** and [Rh(µ-Cl)(cod)]$_2$ (2:1 ratio) in THF (10 mL) showed no reaction even after prolonged reaction times. Nevertheless, after the addition of methanol (1 mL) the immediate formation of a light yellow solution was observed along with dihydrogen evolution. Stirring for 4 h resulted in an orange solution from which the zwitterionic complex [Rh(cod){(MeIm)$_2$CHCOO}] (**11**) was isolated as a shiny orange powder in 63% yield. Under these reaction conditions the base responsible for the deprotonation of the bis-imidazolium salt is likely NaOMe, which is formed by reaction of NaH and MeOH. Although this methodology was successfully employed to prepare [Rh(nbd){(MeIm)$_2$CHCOO}] (**12**), it was ineffective for the synthesis of the iridium complex [Ir(cod){(MeIm)$_2$CHCOO}] (**13**) (Scheme 5).

**Scheme 5.** Synthetic strategies applied to the preparation of zwitterionic [M(diene){(MeIm)$_2$CHCOO}] complexes.
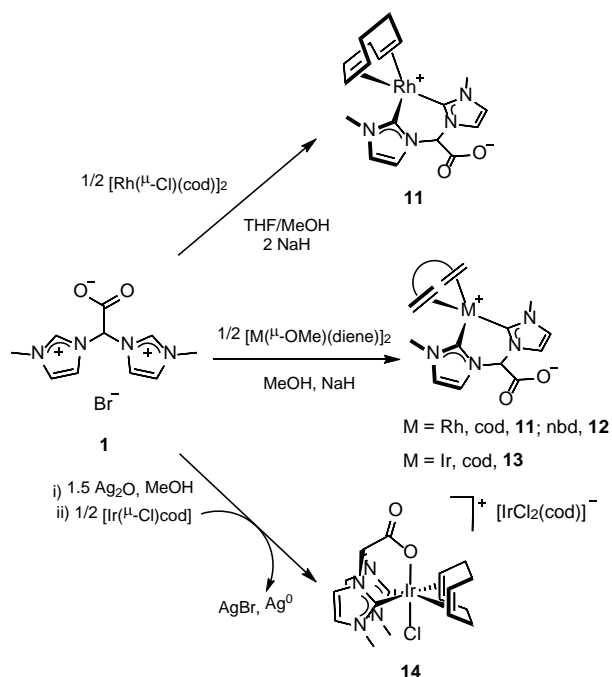
An alternative synthetic protocol for the preparation of **11** entails the sequential reaction of **1** with 0.5 equiv of [Rh(µ-OMe)(cod)]$_2$ and NaH in THF/MeOH which afforded the compound in 75% yield. Most likely, the formation of **11** proceeds through the deprotonation of one of the imidazolium fragments of **1** by the bridging methoxo ligands of the dinuclear compound to give the intermediate [RhBr(cod){(MeIm)(MeImH)CHCOO}] species having a pendant imidazolium fragment which is further deprotonated by NaOMe. This methodology has been successfully applied to the synthesis of [Rh(nbd){(MeIm)$_2$CHCOO}] (**12**) which has been obtained in 73% yield starting from [Rh(µ-OMe)(nbd)]$_2$. Interestingly, the iridium complex [Ir(cod){(MeIm)$_2$CHCOO}] (**13**) has been prepared in MeOH following this synthetic methodology and isolated as a red microcrystalline solid in 70% yield after removing the inorganic salts (Scheme 5).[35]

In the crystal structure of **11** and **12** a distorted square-planar geometry at the metal centre was observed along with a κ^{2}C,C' coordination of the bis-NHC ligand and a *flagpole* carboxylate group. An ORTEP view of **11** and **12** is shown in Figure 4. As for the rings Rh(1)-C(1)-N(5)-C(7)-N(9)-C(11) (**11**) and Rh(1)-C(1)-N(5)-C(7)-N(5)'-C(1)' (**12**), similar interplanar (Table 2), pitch (↗ 1.4°, 3.8°, **11**; 0.5°, **12**) and yaw (↘, 6.9°, 8.6°, **11**; 6.2°, **12**) angles are observed suggesting that the bite angle of cod [85.964(8)°] and nbd [70.27(1)°] has rather poor influence on those parameters. Also, it is worth a mention that interplanar angles in **11** and **12** are bigger than in **9** (Table 2), reasonably as a result of the reduced steric congestion around the metal centre both in **11** and **12**. Like for **3** and **4**, for both **11** and **12** similar carbon-oxygen bond lengths indicate charge delocalization within the COO. A view of intermolecular hydrogen bonds between the carboxylate group and lattice methanol molecules and the related data are given in Figure 4.
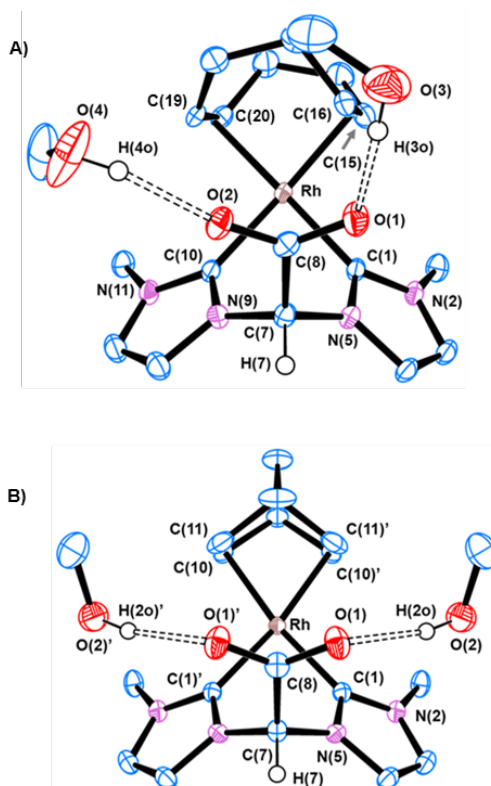
Figure 4. ORTEP view of **11·2CH₃OH** (**A**) and **12·2CH₃OH** (**B**). Ellipsoids are at the 50 % of probability and most hydrogen atoms are omitted for clarity. Selected bond lengths (Å) and angles (°) are: **11**, Rh-C(1) 2.049(2), Rh-C(10) 2.031(2) Rh-ct(1) 2.0781(2), Rh-ct(2) 2.1008(2), C(15)-C(16) 1.379(4), C(19)-C(20) 1.381(4), O(1)-C(8) 1.249(3), O(2)-C(8) 1.246(3), C(1)-Rh-C(10) 83.27(9), ct(1)-Rh-ct(2) 85.964(8), ct(1), centroid of C(15) and C(16), ct(2) centroid of C(19) and C(20). **12**, Rh-C(1) 2.0295(16), Rh-ct 2.0682(2), C(10)-C(11) 1.377(3), O(1)-C(8) 1.2453(17), C(1)-Rh-C(1)' 84.05(9), ct-Rh-ct' 70.27(1); ct/ct', centroid of C(10)/C(10)' and C(11)/C(11)'. Hydrogen bond parameters (Å, °): **11**, O(3)-H(3o) 0.840(2), H(3o)···O(1) 1.859(2), O(1)···O(3) 2.697(3), O(3)-H(3o)-O(1) 174.4(2); O(4)-H(4o) 0.840(3), H(4o)···O(2) 1.882(2), O(4)···O(2) 2.705(3), O(4)-H(4o)-O(2) 166.2(2); **12**, O(2)-H(2o) 0.840(2), H(2o)···O(1) 1.894(1), O(1)···O(2) 2.719(2), O(2)-H(2o)-O(1) 166.9(1). ' symmetry operator +x; ½−y; +z.

Compounds **11-13** have been fully characterized in solution by multinuclear NMR spectroscopy. The ^{1}H NMR spectrum of complex **11** in CD_2Cl_2 evidenced the presence of two symmetrical isomers in a 3.6/1 ratio as two sets of independent resonances can be identified in the spectrum (Figure 5). The functionalized bis-NHC ligand of the major isomer (○) showed two doublets at δ 7.26 and 6.81 ppm with a J_{H-H} of 2.0 Hz for the imidazole-2-carbene protons, and a singlet at δ 6.03 ppm for the -CHCOO resonance. Interestingly, the minor isomer (▲) showed a very different pattern: two well separated doublets at δ 7.95 and 6.69 ppm and a downfield shifted resonance up to δ 7.09 ppm for the methyne. The equivalent N-Me protons of both isomers gave two singlets at δ 3.73 and 3.70 ppm, respectively. Although an averaged broad signal at δ 4.84 ppm is observed for the =CH olefin protons of both isomers (Figure 5), =CH carbons were observed in the [13]C{[1]H} as two sets of doublets at δ 93.9, 86.8 ppm (major isomer) and 91.8, 87.1 ppm (minor isomer), with J_{C-Rh} of ≈ 8.4 Hz, which is in agreement with the presence of a symmetry plane in both isomers. In addition, the downfield doublet at δ 179.5 ppm (J_{C-Rh} = 52.4 Hz) was assigned to the Rh-C_{NCN} resonance of the major isomer, which appears in the range found for related Rh(I)-bis-NHC complexes.[10,11]
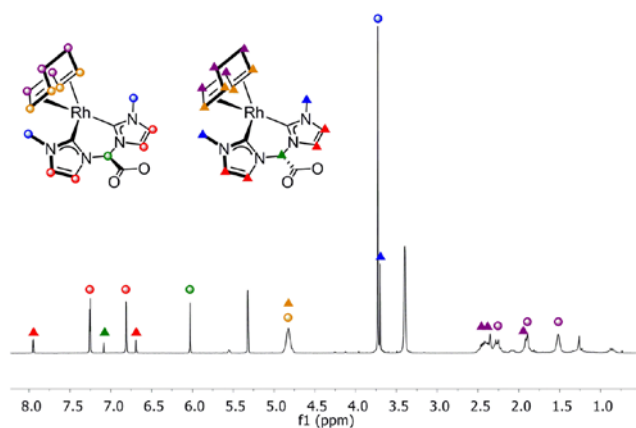
Figure 5. ^{1}H NMR (CD_2Cl_2, 298 K) spectrum of [Rh(cod){(MeIm)_2CHCOO}] (**11**).

The presence of two isomers for **11** is likely related with the different disposition of the carboxylate moiety in the 6-membered metallacycle exhibiting a boat conformation. The major species is the *flagpole* isomer as inferred by the [1]H-[1]H-NOESY spectrum that showed a weak proximity cross peak between the methyne resonance and that of the adjacent =CH protons of the imidazole-2-carbene rings at δ 6.03 and 7.26 ppm, respectively (see Supporting Information). Thus, the carboxylate fragment occupies a *flagpole* position in the major isomer, as it has been found in the solid-state structure, and a *bowsprit* position in the minor isomer. The methyne proton in the minor isomer is pointing to the metal centre over the metallacycle which strongly influences the chemical shift of the -CHCOO resonance. This resonance has been found downfield shifted up to δ 7.09 ppm in the *bowsprit* isomer whereas it is observed at δ 6.03 ppm in the *flagpole* isomer, which could be a consequence of an anagostic interaction H···Rh with the metal centre.[45,46,47] The H···Rh distance of 2.908 Å calculated for the *bowsprit* isomer lies in the upper range of distances observed for anagostic interactions and is much shorter than that found in the *flagpole* isomer (4.142 Å).[45]

Molecular models show that both stereoisomers can interconvert by inversion of the 6-membered metallacycle ring. Accordingly strong exchange cross-peaks between the -CHCOO resonances at δ 7.09 and 6.03 ppm as well as between those resonances corresponding to the =CH of the imidazole-2-carbene rings appear in the ^{1}H-^{1}H-NOESY NMR spectrum of **11**, which indicate that both isomers actually interconvert in solution (Figure 6).
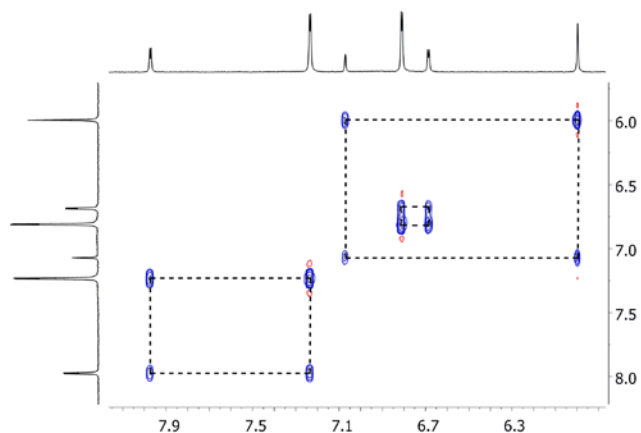
Figure 6. [1]H-[1]H-NOESY (CD_2Cl_2, 300 K) spectrum of [Rh(cod){(MeIm)_2CHCOO}] (**11**).

^{1}H 2D-EXSY NMR measurements were carried out to determine the forward and backward rate constants k_1 and k_{-1} for the equilibrium between both conformational isomers of **11** (Figure 7, see Supporting Information).[48] Notably, the resulting activation barriers ($\Delta G^{\ddagger}_{1,300\ K}$ = 18.1 kcal·mol^{-1}; $\Delta G^{\ddagger}_{-1,300\ K}$ = 16.7 kcal·mol^{-1}) nicely fit in with the activation barrier determined for the boat-to-boat inversion in mononuclear palladium(II) complexes featuring methylene-bridged 1,2,4-triazole-derived bis-NHC ligands.[49] The equilibrium constant K_{EXSY} obtained from the determined rate constants is in good agreement with the experimental value of K_{Int}, obtained from the same sample by integration of the =CH resonances of the imidazole-2-carbene rings in an experiment recorded with the same relaxation time.
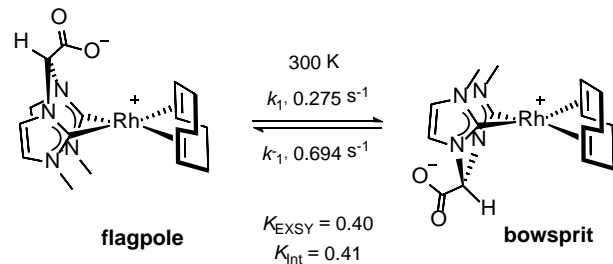
Figure 7. [1]H 2D-EXSY derived rate constants (k_1 and k_{-1} in s[-1]) and calculated equilibrium constant (K) for the equilibrium between the *flagpole* and *bowsprit* isomers of compound **11**.

A variable temperature ^{1}H NMR study in the temperature range of 231-295 K also supports the existence of a dynamic equilibrium between both isomers. The equilibrium constant K = [*bowsprit*]/[*flagpole*], is 0.34 at 295 K and decreases to 0.09 at 231 K, pointing at an endothermic character of the inversion. Indeed the thermodynamic parameters of the inversion determined by means of a Van't Hoff plot[50] are: ΔH^o = 2.7 ± 1.2 kcal·mol^{-1} and ΔS^o = 6.6 ± 1.1 cal·K^{-1}·mol^{-1} (see Supporting Information).

Unexpectedly, the ^{1}H NMR spectrum of **11** recorded in CD$_3$OD showed only one isomer which is indicative of the strong influence of the solvent on the equilibrium. The observed pattern for the =CH imidazole-2-carbene resonances and the two broad resonances for the =CH cod olefin protons is in agreement with the presence of the *flagpole* isomer of C_s symmetry. A variable temperature ^{1}H NMR study in CD$_3$OD showed exclusively the presence of the *flagpole* isomer in the range of temperature from 213 to 328 K.

The ^{1}H NMR spectrum of [Rh(nbd){(MeIm)$_2$CHCOO}] (**12**) in CD$_2$Cl$_2$ at room temperature showed a singlet at δ 6.16 ppm for the methyne proton and a broad signal at 4.85 ppm for the four vinyl =CH protons of the nbd ligand. Also, the =CH carbons were also observed as a broad resonance at δ 79.4 ppm in the ^{13}C{^{1}H} NMR spectrum which suggests a dynamic behavior. The ^{1}H NMR spectrum of **12** recorded in CD$_2$Cl$_2$ at 233 K also showed the presence of the *bowsprit* isomer with a *flagpole*/*bowsprit* ratio of 5/1 (K = 0.20). The =CH imidazole-2-carbene protons of the *bowsprit* isomer appeared as two overlapped signals rendering an apparent triplet at δ 6.72 ppm (J_{H-H} = 1.9 Hz) whereas the CHCOO resonance is seen as a singlet significantly downfield shifted up to δ 7.34 ppm compared to that of the major *flagpole* stereoisomer which is observed at 6.16 ppm (see Supporting Information). The easy interconversion of both isomers at room temperature suggests a low energy barrier for the boat-to-boat inversion process which is in agreement with the presence of the less steric demanding nbd ligand in **12** compared to cod.

Similar to the related rhodium compound **11**, compound [Ir(cod){(MeIm)$_2$CHCOO}] (**13**) exists in CD$_3$OD as the *flagpole* isomer in the temperature range 298-213 K as shown by the ^{1}H NMR spectra.[35] Unfortunately, the ^{1}H NMR spectrum in CD$_2$Cl$_2$ showed featureless resonances even at 213 K which makes difficult the structural assignment in this solvent.

In order to determine the relative stability of the two possible isomers for complexes **11-13**, the corresponding structures have been optimized by DFT calculations performed in both solvents, CH$_2$Cl$_2$ and MeOH. In agreement with the experimental observations, the *flagpole* isomer is always more stable than the *bowsprit* isomer (Table 4).

Table 4. Calculated Gibbs free energy differences ΔG = $G_{bowsprit}$ − $G_{flagpole}$ for [M(diene){(MeIm)$_2$CHCOO}] and [M(cod)(LMe)]$^+$ (M = Rh, Ir), L = (MeIm)$_2$CHCOO in methanol, dichloromethane and gas phase.

	ΔG (kcal·mol^{-1})		
	MeOH	CH$_2$Cl$_2$	Gas
[Rh(cod){(MeIm)$_2$CHCOO}] (**11**)	1.82	1.57	2.29
[Rh(nbd){(MeIm)$_2$CHCOO}] (**12**)	1.42	0.50	2.46
[Ir(cod){(MeIm)$_2$CHCOO}] (**13**)	0.98	0.86	0.74
[Rh(cod)(LMe)]OTf (**15**)	5.15	5.12	2.76
[Ir(cod)(LMe)]OTf (**16**)	5.41	5.24	3.30

The DFT calculations showed no large differences in terms of energy between both isomers of complexes **11-13** derived from the ligand (MeIm)$_2$CHCOO$^-$ in both solvents. The observation of both isomers in dichloromethane solutions of complexes **11** and **12** is in accordance with their small energy difference. However, only the *flagpole* isomer is found in CD$_3$OD solutions of **11** and **13**. Most likely, the interaction of methanol molecules with the carboxylate moiety prevents the inversion of the 6-membered metallacycle ring by increasing the energy barrier for the inversion of the metallacycle and therefore the *bowsprit* isomer is not seen.

Palladium(II)–bis(NHC) complexes derived from *N,N*-bis(1,2,4-triazol-1-yl)methane bearing an hydroxyl-alkyl chain substituent at the bridge also show a non-equimolecular mixture of two interconverting isomers in solution with the *flagpole* species as the predominant one. Theoretical calculations on a simplified model have also shown that the *flagpole* isomer is slightly more stable (1–3 kcal·mol^{-1}) than the *bowsprit* isomer.[26,51] However, it is worth mentioning that the uncoordinated pyrazol ring of square planar palladium(II) complexes featuring a tris(pyrazol-1-yl)borate ligand κ^2*N,N'* coordinated is located at a *bowsprit* position of the palladacycle.[52]

The use of silver-carbene as transfer agents for the synthesis of iridium(I) complexes could be considered a challenge due to the possible oxidation of metal centre. In fact, reaction of [(MeIm)$_2$CHCOOAg]$_2$ (**2**) with the dinuclear complexes [M(μ-Cl)(cod)]$_2$ (M = Rh, Ir) leads to an untreatable mixture of unidentified compounds. However, when the reaction of [Ir(μ-Cl)(cod)]$_2$ with **2**, generated *in situ* in methanol, was conducted in the presence of a moderate excess of Ag$_2$O the the ion-pair [IrCl(cod){(MeIm)$_2$CHCOO}][IrCl$_2$(cod)] (**14**) was isolated as a yellow solid in moderate yield (Scheme 5).

As observed in the solid state structure of **14**, the square planar anion [IrCl$_2$(cod)]$^-$ is similar to that already described for related compounds (see Supporting Information).[53,54,55] The iridium(III) cation [IrCl(cod){κ^3*C,C',O*-(MeIm)$_2$COO}]$^+$ in **14** exhibits a distorted octahedral coordination polyhedron with a κ^3*C,C',O* coordination mode of the tridentate bis-NHC ligand. The coordination sphere is completed by the bidentate cod ligand and one chlorido, *trans* to the oxygen atom [O(1)-Ir(1)-Cl(1) 168.15(13)°, Figure 8]. As for the cod and bis-NHC ligands, bond lengths and angles are similar to those reported for the related hydrido derivative [IrH(cod){κ^3*C,C',O*-(MeIm)$_2$COO}]$^+$.[35] Notably as a consequence of the κ^3*C,C',O* coordination of the bis-NHC ligand, the interplanar angles (Table 2) of the 6-member ring Ir-C(1)-N(5)-C(7)-N(9)-C(10) as well as the yaw angles {⅄ 9.8, C(1); 9.0, C(10)} of the imidazole-2-carbene moieties are bigger than those of the related rhodium(I) derivative **11** (*vide supra*) and of the previously reported[35] complex Ir(cod){κ^2*C,C'*-(MeIm)$_2$COO}.

The mass spectrum and the spectroscopic data for **14** are in agreement with the structure found in the solid state. The ^{1}H NMR spectrum of **14** in CD$_3$OD showed two doublets at δ 6.81 and 5.94 (J_{H-H} = 2.1 Hz) for the =CH imidazole-2-carbene protons, and two well separate resonances at δ 5.90 and 4.67 ppm for the =CH olefin protons of the cod ligand, in agreement with the C_s symmetry of the cation. On the other hand, the κ^3*C,C',O* coordination of the carboxylate-funtionalized bis-NHC ligand results in a significant downfield shift of the -CHCOO resonance up to δ 6.99 ppm which is a diagnostic for this coordination mode. Furthermore, the C$_{NCN}$ resonance was found at δ 135.4 ppm in the ^{13}C{^{1}H} NMR spectrum (CD$_3$OD), considerably high-field shifted compared to that of **13** (176.2 ppm) in agreement with the oxidation of the iridium center.[22,56,57] The ATR-IR spectrum show an intense absorption at 1694 cm^{-1} corresponding to the asymmetric stretching COO band of the coordinated carboxylate fragment, at higher energy than in the zwitterionic complex **13** (1648 cm^{-1}).
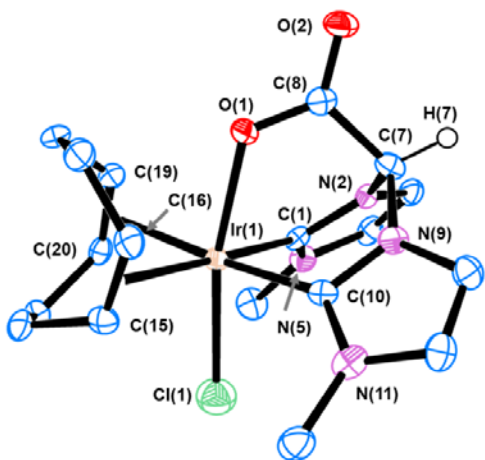
Figure 8. ORTEP view of the cation [IrCl(cod){κ^3C,C',O-(MeIm)2COO}]$^+$ in **14**. Ellipsoids are at the 50 % of probability and most hydrogen atoms are omitted for clarity. Selected bond lengths (Å) and angles (°) are: Ir(1)-C(1) 2.032(6), Ir(1)-C(10) 2.017(6), Ir(1)-O(1) 2.127(4), Ir(1)-Cl(1) 2.373(2), Ir(1)-ct(1) 2.2316(4), Ir(1)-ct(2) 2.2217(5), C(15)-C(16) 1.376(9) C(19)-C(20) 1.378(9), O(1)-C(8) 1.293(8) O(2)-C(8) 1.224(8) C(1)-Ir(1)-C(10) 84.3(2) O(1)-Ir(1)-Cl(1) 168.21(13) ct(1)-Ir(1)-ct(2) 81.28(2) C(1)-Ir(1)-O(1) 85.8(2) C(10)-Ir(1)-O(1) 84.9(2). ct(1), centroid of C(15) and C(16); ct(2), centroid of C(19) and C(20).

In order to verify that the ion Ag$^+$ is the actual oxidant of the iridium(I) centre in the formation of **14**, the reactivity of [Ir(cod){(MeIm)$_2$CHCOO}] (**13**) with silver(I) salts was explored. Two step reaction of **13** with AgBF$_4$ (2 equiv) in methanol and NaCl gave a dark suspension. Interestingly, the ^{1}H NMR of the yellow solution obtained after removing the inorganic solids showed the presence of unreacted **13** and the iridium(III) cations [IrH(cod){(MeIm)$_2$CHCOO}]$^{+,35}$ and [IrCl(cod){(MeIm)$_2$CHCOO}]$^+$, which confirms the role of the excess of Ag$_2$O in the synthesis of **14**.

Reactivity of zwitterionic [M(cod){(MeIm)$_2$CHCOO}] (M = Rh, Ir) complexes with electrophiles. The uncoordinated carboxylate fragment in the zwitterionic complexes [M(cod){(MeIm)$_2$CHCOO}] (M = Rh, Ir) is a nucleophilic site and therefore can react with electrophiles to give the corresponding M(I) cationic complexes. Nevertheless, due to the presence of the strong electron donating bis-NHC ligand the direct attack of the electrophile to the basic M(I) metal centre, to give cationic octahedral M(III) complexes cannot be ruled out.

The addition of MeOTf to solutions of the water soluble complexes [M(cod){(MeIm)$_2$CHCOO}] (M = Rh, **11**; Ir, **13**) in dichloromethane afforded the compounds [M(cod){(MeIm)$_2$CHCOOMe}]OTf (M = Rh, **15**; Ir, **16**) which were isolated as dark orange-red solids in good yields (Scheme 6). The ^{1}H and ^{13}C{^{1}H} NMR spectra in CD$_2$Cl$_2$ showed the characteristic singlet resonances for the methyl group of the methoxycarbonyl fragment at δ 3.89 and 54.4 (**15**), and 3.83 and 54.3 ppm (**16**). Also, the spectra of both complexes show a similar pattern of resonances and the presence of a single isomer of C_s symmetry. In particular, the methyne resonance at δ 7.29 (**15**) and 7.15 (**16**) ppm in the ^{1}H NMR spectra, significantly downfield shifted compared to that of the parent complexes, suggests the location of the methoxycarbonyl fragment in *bowsprit*

position allowing for the CH···M interaction. However, the ^{1}H-^{1}H-NOESY spectrum of **15** evidenced the existence of the *flagpole* isomer as proximity cross peaks between the methoxycarbonyl fragment and one of the =CH of the cod ligand (δ 3.89 and 4.69 ppm, respectively), and the -CHCOO resonance and the adjacent =CH protons of the imidazole-2-carbene rings (δ 7.29 and 7.67 ppm, respectively) were observed (see Supporting Information). Furthermore, DFT calculations also predict the higher stability of the *flagpole* isomer by ~5 Kcal·mol^{-1} for both compounds, in both solvents (Table 4). A variable temperature NMR study exclusively showed the *flagpole* isomer in the temperature range of 183-313 K.

Scheme 6. Reactivity of zwitterionic [M(cod){(MeIm)$_2$CHCOO}] (M = Rh, Ir) complexes with MeOTf and HBF$_4$.
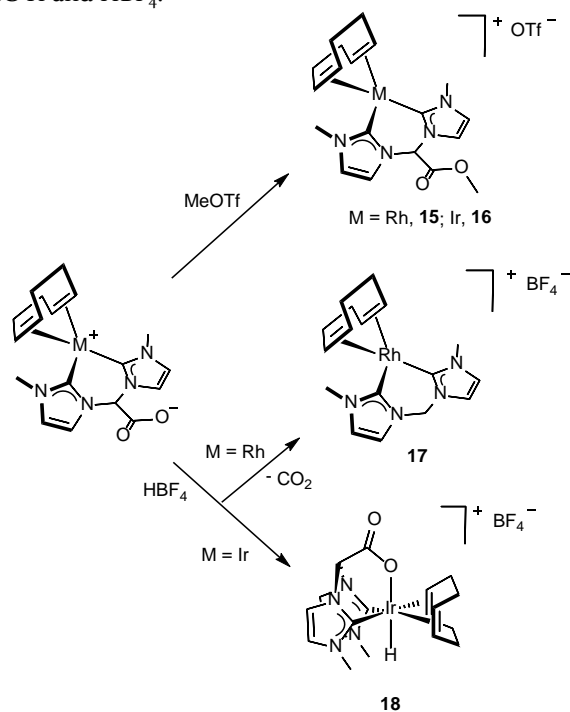
Reaction of zwitterionic [Rh(cod){(MeIm)$_2$CHCOO}] (**11**) with HBF$_4$·Et$_2$O in CH$_2$Cl$_2$ resulted in the unexpected decarboxylation of the complex with the formation of the ionic compound [Rh(cod){(MeIm)$_2$CH$_2$}]BF$_4$ (**17**) and CO$_2$(g) (Scheme 6). The compound has been characterized by comparison of the spectroscopic properties with those of the iodide salt prepared following the procedure described by Herrmann *et al.*[58] In sharp contrast, reaction of [Ir(cod){(MeIm)$_2$CHCOO}] (**13**) with HBF$_4$·Et$_2$O in dichloromethane at 223 K afforded a yellow solution of the cation [IrH(cod){(MeIm)$_2$CHCOO}]$^+$ which is supposed to be formed by direct protonation of the iridium centre. The compound was isolated as the tetrafluoroborate salt [IrH(cod){(MeIm)$_2$CHCOO}]BF$_4$ (**18**) in 72% yield. The formation of the cationic hydrido iridium(III) species was confirmed by comparison of the ^{1}H NMR spectrum in DMSO-d_6 with that of the triflate salt that showed the characteristic high-field singlet at δ -19.05 ppm for the hydrido ligand.[35]

The presence of an electron rich iridium(I) centre in [Ir(cod){(MeIm)$_2$CHCOO}] (**13**) prompted us to explore oxidative addition reactions with the aim of preparing octahedral iridium(III) complexes stabilized by the κ^3*C,C',O* coordination of the carboxylate-functionalized bis-NHC ligand. Stirring of a red suspension of **13** in neat MeI gave a yellow suspension of complex [Ir(CH$_3$)(cod){(MeIm)$_2$CHCOO}]I (**19**) which was isolated as a yellow solid in 79% yield (Scheme 7).

Scheme 7. Reactivity of zwitterionic [Ir(cod){(MeIm)$_2$CHCOO}] (**13**) complex with MeI and I$_2$.
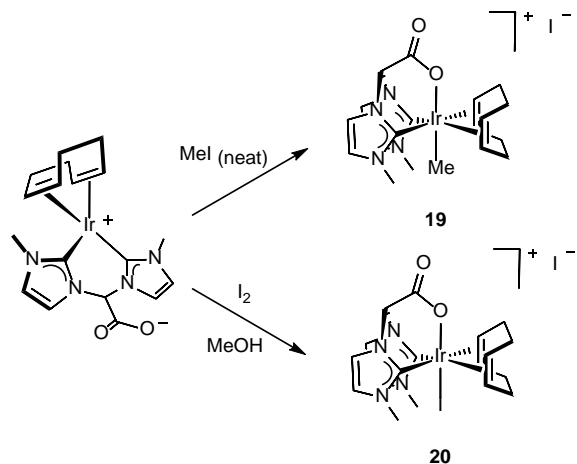
The ionic character of the compound was also confirmed by the measurement of the conductivity which is in the expected range for a 1:1 electrolyte (83.2 Ω^{-1}·cm^2·mol^{-1} in methanol).[59] The ^{1}H and ^{13}C{^{1}H}-apt NMR spectra also confirmed the formation of the Ir-CH$_3$ bond and the κ^3*C,C',O* coordination of the carboxylate-functionalized bis-NHC ligand. The methyl ligand gave a singlet at δ 1.58 ppm in the ^{1}H NMR spectrum and at δ -29.5 ppm in the ^{13}C{^{1}H}-apt spectrum.[60] The imidazole-2-carbene rings protons were observed as a set of two doublets and the methyne resonance as a singlet at δ 6.83 ppm. These resonances were found downfield shifted compared to that of the parent zwitterionic iridium(I) complex **13** (Figure 9) but roughly at the same chemical shift as in the cationic hydrido iridium(III) compound **18**. Interestingly, all these features are diagnostic of the κ^3*C,C',O* coordination mode of the carboxylate-functionalized bis-NHC ligand. In addition, the cod ligand exhibits two well separate resonances for the =CH olefin protons at δ 6.03 and 5.22 ppm, also largely downfield shifted compared to that of **13**, as a consequence of the oxidation of the iridium centre. Similarly to compound **18**, the equivalent C$_{NCN}$ carbon atoms were observed at δ 147.3 ppm in the ^{13}C{^{1}H} NMR spectrum.

The addition of solid I$_2$ to a red solution of [Ir(cod){(MeIm)$_2$CHCOO}] (**13**) in MeOH gave a yellow solution after 10 minutes of vigorous stirring from which complex [IrI(cod){(MeIm)$_2$CHCOO}]I (**20**) was isolated as a yellow solid in 87% yield (Scheme 7). The ionic character of the compound was established by conductivity measurement, that lies in the expected range for a 1:1 electrolyte (84.7 Ω^{-1}·cm^2·mol^{-1}, methanol), and the ESI+ mass spectra that showed a peak at *m/z* 647.0 with the expected isotopic distribution for the cation [IrI(cod){(MeIm)$_2$CHCOO}]$^+$. Moreover, the ^{1}H and ^{13}C{^{1}H}-apt NMR spectra are in agreement with the presence of a functionalized bis-NHC ligand κ^3*C,C',O*-coordinated.

Thus, the oxidative addition reactions on **13** result in formation of iridium(III) complexes in which only the electrophilic fragment of the reagent becomes coordinated to the metal centre, and the carboxylate fragment of the functionalized bis-NHC ligand eventually completes the coordination sphere of the metal.
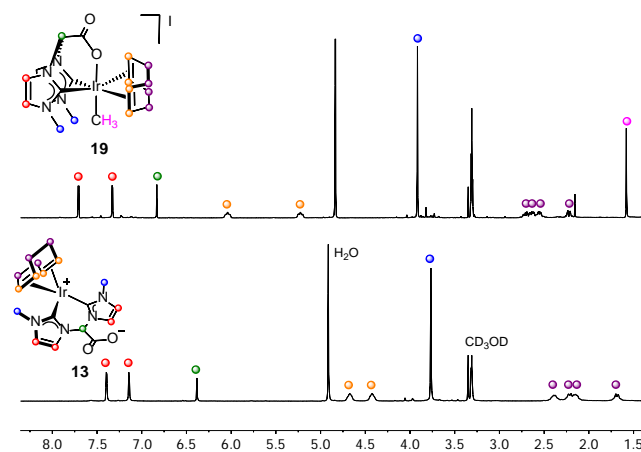
Figure 9. ^{1}H NMR (CD$_3$OD, 298 K) spectra of [Ir(CH$_3$)(cod){(MeIm)$_2$CHCOO}]I (**19**) and the parent iridium(I) complex [Ir(cod){(MeIm)$_2$CHCOO}] (**13**).

Table 5 summarizes the -CHCOO, C$_{NCN}$ and COO chemical shifts observed in the ^{1}H and ^{13}C{^{1}H} NMR spectra of **13** and the iridium(III) complexes derived from it. The methyne resonance, sensitive to the coordination mode of the ligand, is also influenced by the coordinated atom *trans* to the Ir-O bond. Further, the C$_{NCN}$ resonance in the ^{13}C{^{1}H} NMR spectra, strongly influenced by the increase of the oxidation state of the iridium centre, is also sensitive to the ligand trans to the carboxylate moiety. Finally, the chemical shift of the COO resonance is much less sensitive to the changes in the coordination sphere of the iridium centre.

Table 5. Selected ^{1}H and ^{13}C NMR chemical shifts of selected iridium(I) and iridium(III) complexes (CD$_3$OD at 298 K).[a,b]

Complex	CHCOO	C$_{NCN}$	COO
[Ir(cod)L] (**13**)	6.38	176.2	170.1
[IrCl(cod)L][IrCl$_2$(cod)] (**14**)	6.99	135.4	166.0
[IrH(cod)L]X (**18**)[c]	6.89	149.6	163.8
[IrMe(cod)L]I (**19**)	6.83	147.3	168.0
[IrI(cod)L]I (**20**)	7.01	134.3	165.9

[a] L = (MeIm)$_2$CHCOO; [b] δ ppm; [c] NMR spectra in DMSO-d_6.

CONCLUSIONS

The salt 1,1'-bis(*N*-methylimidazolium)acetate bromide is a suitable precursor for the preparation of water-soluble zwitterionic rhodium and iridium complexes featuring a carboxylate bridge-functionalized bis-N-heterocyclic carbene ligand. The [Cp*M^{III}Cl{(MeIm)2CHCOO}] (M = Rh, **3**, Ir, **4**) complexes have been prepared following the silver-NHC transmetallation strategy whereas the synthesis of complexes [M^I(diene){(MeIm)2CHCOO}] (M = Rh, Ir, diene = cod, nbd,

11 - 13) has been accomplished by the in situ deprotonation of the functionalized bis-imidazolium salt methodology. The bis-NHC ligand in both types of compounds exhibits a κ2*C,C'* coordination mode with an uncoordinated carboxylate group that imparts water solubility to the complexes.

The solid state structure of Cp*M^{III} zwitterionic complexes show a boat-shaped 6-membered metallacycle with the uncoordinated carboxylate fragment at the *bowsprit* position. In contrast, the solid state structure of M^{I}(diene) complexes showed the carboxylate fragment at the *flagpole* position of the metallacycle. The Cp*M^{III} complexes exist as a single isomer in solution although both conformational isomers, *bowsprit* and *flagpole*, were observed in dichloromethane solutions of complexes [Rh^{I}(diene){(MeIm)$_2$CHCOO}] (diene = cod, nbd). NMR studies evidenced the existence of a dynamic equilibrium between both isomers that involves a boat-to-boat inversion of the metallacycle. An inversion barrier of around 17 kcal·mol^{-1} has been determined by 2D EXSY NMR measurements for [Rh^{I}(cod){(MeIm)$_2$CHCOO}].

The uncoordinated carboxylate fragment in these complexes is reactive towards electrophiles such as H$^+$ and Me$^+$ which have allowed the synthesis of cationic complexes featuring carboxy- and methoxycarbonyl functionalized methylene-bridged bis-NHC ligands. Thus, complexes [Cp*M^{III}Cl{(MeIm)$_2$CHCOOMe}]$^+$ (M = Rh, **5**, Ir, **6**) and [Cp*M^{III}Cl{(MeIm)$_2$CHCOOH}]$^+$ (M = Rh, **7**, Ir, **8**) were prepared by reaction of the corresponding carboxylated-functionalized complexes with methyl triflate and tetrafluoroboric acid, respectively. Remarkably, chlorido abstraction from [Cp*Rh^{III}Cl{(MeIm)$_2$CHCOOMe}]$^+$ by silver triflate triggers a conformational change in the metallacycle that results in the shift of the methoxycarbonyl moiety from *bowsprit* to *flagpole* in **9** and **10**.

In the same way, complexes [M^{I}(diene){(MeIm)$_2$CHCOOMe}]$^+$ (M = Rh, **15**, Ir, **16**) have been prepared by alkylation of the corresponding zwitterionic complexes with methyl triflate. Both complexes exist in solution exclusively as the flagpole isomer. On the other hand, the reaction of [Ir^{I}(cod){(MeIm)$_2$CHCOO}] with a range of electrophiles/oxidants such as HBF$_4$·Et$_2$O, HOTf, MeOTf, CH$_3$I or I$_2$, affords cationic iridium(III) octahedral [Ir^{III}X(cod){(MeIm)$_2$CHCOO}]$^+$ (X = H, **18**, Me, **19** or I, **20**) complexes featuring a facial κ^3*C,C',O*-tridentate coordination mode of the functionalized bis-NHC ligand. Coordination of the hard donor carboxylate oxygen in the octahedral Ir(III) reaction products traps the cationic intermediate resulting from nucleophilic attack by Ir(I) on the electrophilic reagents. As a consequence, the displaced anions remain as counterions instead of coordinating to iridium center. New catalytic applications of these unusual complexes are being currently investigated in our laboratories and will be reported in due course.

EXPERIMENTAL SECTION

Synthesis. All the experimental procedures were performed under argon atmosphere by using schlenk or glovebox techniques. Solvents were taken under argon atmosphere from an Innovative Technologies PS-400-6 solvent purification system (SPS) or dried following standard procedures and distilled under argon prior to use.[61] Standard literature procedures were used to prepare the starting materials [Ir(μ-Cl)(cod)]$_2$,[62] [Rh(μ-Cl)(diene)]$_2$ (diene = cod, nbd),[63] [Ir(μ-OMe)(cod)]$_2$, [Rh(μ-OMe)(cod)]$_2$,[64] [Rh(μ-OMe)(nbd)]$_2$,[65] [Cp*IrCl$_2$]$_2$, and [Cp*RhCl$_2$]$_2$ (Cp* = η^5-C$_5$Me$_5$).[66] 1,1'-Bis(N-methylimidazole)acetate bromide, [(MeImH)$_2$CHCOO]Br (**1**), was prepared from 1-methylimidazole (MeImH) and ethyl dibromoacetate following the procedure recently described by us.[35] Deuterated solvents CDCl$_3$ and CD$_2$Cl$_2$ (Euriso-top) were dried using activated molecular sieves and degassed by three freeze-pump-thaw cycles. CD$_3$OD (<0.02% D$_2$O) was purchased from Euriso-top and used as received.

Scientific Equipment ^{1}H, ^{13}C{^{1}H}, ^{19}F and ^{31}P{^{1}H} NMR spectra were recorded on Bruker Avance-300, Avance-400 and Avance-500 spectrometers or on a Varian Inova-300 spectrometer. Chemical shifts are reported in ppm relative to tetramethylsilane and coupling constants (*J*) are given in Hertz (Hz). The ^{1}H and ^{13}C{^{1}H} spectra were referenced using the residual solvent signal as internal standard, while ^{19}F and ^{31}P{^{1}H} spectra were referenced to CFCl$_3$ and H$_3$PO$_4$ (85%), respectively. Assignment was performed, when necessary, with the following 2D-NMR experiments: ^{1}H-^{1}H gradient-selected correlation spectroscopy (gCOSY), ^{1}H-^{13}C heteronuclear single quantum coherence (HSQC), ^{1}H-^{13}C heteronuclear multiple bond correlation (HMBC) and ^{1}H-^{1}H nuclear Overhauser enhancement spectroscopy (NOESY). Electrospray Ionization (ESI) mass spectra were recorded using a Bruker Esquire3000 plus™ ion-trap mass spectrometer equipped with a standard ESI source. Samples were introduced on a continuous flow of 0.2 mL/min. Nitrogen served both as the nebulizer and dry gas. High-resolution mass spectra-ESI (HRMS-ESI) were recorded using a Bruker MicroToF-Q™ equipped with an API-ESI source and a Q-ToF mass analyser, which leads a maximum error in the measurement of 5 ppm. Acetonitrile and methanol were used as solvents. Samples were introduced on a continuous flow of 0.2 mL/min. Nitrogen served both as the nebulizer and dry gas. Conductivities (Λ$_M$) were measured at room temperature in *ca*. 5·10^{-4} M acetone, methanol or nitromethane solutions on a Philips PW9501/01 Conductivity Meter. Infrared spectra were recorded on a 100 FTIR-Perkin-Elmer Spectrophotometer equipped with a Universal Attenuated Total Reflectance (UATR) accessory made by thallium bromide-iodide crystals (KRS-5), which allows the observation of the electromagnetic spectrum over the 4000-250 cm^{-1} region. C, H and N analyses were carried out in a Perkin-Elmer 2400 Series II CHNS/O analyzer.

Synthesis of the complexes. [(MeIm)$_2$CHCOOAg]$_2$ (2). Ag$_2$O (149.3 mg, 0.644 mmol) was added to a solution of [(MeImH)$_2$CHCOO]Br (**1**) (194 mg, 0.644 mmol) in CH$_2$Cl$_2$/MeOH (10 mL, 1:1, v:v). The mixture was stirred for 16 hours in the dark and then filtered via cannula through Celite to remove the AgBr formed. The pale yellow solution was kept in the absence of light and concentrated under vacuum to give a white suspension which was decanted. The white powder was washed with diethyl ether and dried under vacuum. Yield: 183.2 mg, 86%. Anal. Calc. for C$_{20}$H$_{22}$Ag$_2$N$_8$O$_4$·CH$_3$OH: C 36.76; H, 3.82; N, 16.33. Found: C 36.49; H, 3.70; N, 16.29. ^{1}H NMR (298 K, 300 MHz, CD$_3$OD): δ 7.76 (s, 2H, CHCOO), 7.68 (br, 4H, CH), 7.32 (br, 4H, CH), 3.91 (s, 6H, NCH$_3$), 3.90 (s, 6H, NCH$_3$). MS (ESI+, DMSO/MeOH, *m/z*, %): 654.0 ([M]$^+$, 100), 567.0 ([M-2COO+H]$^+$, 35). IR (ATR, cm^{-1}): 1665 (COO).

[Cp*RhCl{(MeIm)$_2$CHCOO}] (3). [Cp*RhCl$_2$]$_2$ (292.3 mg, 0.473 mmol) was added to a solution of [(MeIm)$_2$CHCOOAg]$_2$ (**2**) (309.4 mg, 0.473 mmol) in CH$_2$Cl$_2$/MeOH (10 mL, 1:1, v:v) in the absence of light. The suspension was stirred for 6 hours

and then filtered via a cannula through Celite to remove the AgCl formed. Then, the resulting solution was concentrated to *ca.* 1 mL under reduced pressure. Slow addition of diethyl ether afforded the solids as an intense yellow solid which was filtered, washed with diethyl ether (3 x 3 mL) and dried in vacuo. Yield: 435.9 mg, 93%. Anal. Calc. for $C_{20}H_{26}ClN_4O_2Rh \cdot CH_3OH$: C, 48.06; H, 5.76; N, 10.67. Found: C, 47.66; H, 5.65; N, 10.51. ^{1}H NMR (298 K, 300 MHz, $CDCl_3$): δ 7.94 (d, J_{H-H} = 2.1, 2H, CH), 6.98 (d, J_{H-H} = 2.1, 2H, CH), 5.83 (s, 1H, CHCOO), 3.85 (s, 6H, NCH_3), 1.71 (s, 15H, CH_3 Cp*). $^{13}C\{^1H\}$ NMR (298 K, 75 MHz, $CDCl_3$): δ 168.0 (d, J_{C-Rh} = 50.7, C_{NCN}), 163.3 (COO), 123.4, 122.6 (CH), 99.5 (d, J_{C-Rh} = 5.3, CCH_3 Cp*), 74.6 (CHCOO), 37.8 (NCH_3), 9.9 (CH_3 Cp*). MS (ESI+, CH_2Cl_2/MeOH, *m/z*, %): 492.1 ([M+H]$^+$, 100). IR (ATR, cm^{-1}): 1650 (COO).

[Cp*IrCl{(MeIm)$_2$CHCOO}] (4). [Cp*IrCl$_2$]$_2$ (256.5 mg, 0.322 mmol) and [(MeIm)$_2$CHCOOAg]$_2$ (2) (210.6 mg, 0.322 mmol) in CH_2Cl_2/MeOH (10 mL, 1:1, v:v). Work up as described above gave the compound as a pale yellow solid. Yield: 298.7 mg, 80%. Anal. Calc. for $C_{20}H_{26}ClIrN_4O_2 \cdot CH_3OH$: C 41.07; H, 4.92; N, 9.12. Found: C 40.75; H, 4.88; N, 9.17. ^{1}H NMR (298 K, 300 MHz, CD_2Cl_2): δ 7.82 (d, J_{H-H} = 2.1, 2H, CH), 6.99 (d, J_{H-H} = 2.1, 2H, CH), 5.72 (s, 1H, CHCOO), 3.80 (s, 6H, NCH_3), 1.79 (s, 15H, CH_3 Cp*). $^{13}C\{^1H\}$ NMR (298 K, 75 MHz, CD_2Cl_2): δ 163.7 (COO), 151.4 (C_{NCN}), 122.5, 122.4 (CH), 93.3 (CCH_3 Cp*), 75.5 (CHCOO), 37.5 (NCH_3), 9.8 (CH_3 Cp*). MS (ESI+, CH_2Cl_2/MeOH, *m/z*, %): 583.1 ([M+H]$^+$, 100). IR (ATR, cm^{-1}): 1655 (COO).

[Cp*RhCl{(MeIm)$_2$CHCOOH}]BF$_4$ (5). HBF$_4 \cdot$OEt$_2$ (19.0 μL, ρ = 1.19 g·mL^{-1}, 0.140 mmol) was added to a solution of [Cp*RhCl{(MeIm)$_2$CHCOO}] (3) (61.5 mg, 0.125 mmol) in CH_2Cl_2 (5 mL). The solution was stirred for 30 minutes at room temperature and then was brought to dryness under vacuum. The light yellow solid was washed with cold diethyl ether (3 x 3 mL) and dried under vacuum. Yield: 67.1 mg, 92%. Anal. Calc. for $C_{20}H_{27}BClF_4N_4O_2Rh$: C, 41.37; H, 4.69; N, 9.65. Found: C, 41.18; H, 4.58; N, 9.73. ^{1}H NMR (298 K, 300 MHz, $CDCl_3$): δ 7.68 (d, J_{H-H} = 1.8, 2H, CH), 7.09 (d, J_{H-H} = 1.8, 2H, CH), 6.12 (s, 1H, CHCOO), 4.14 (s, 1H, OH), 3.91 (s, 6H, CH_3), 1.77 (s, 15H, CH_3 Cp*). $^{13}C\{^1H\}$ NMR (298 K, 75 MHz, $CDCl_3$): δ 169.4 (d, J_{C-Rh} = 51.5, C_{NCN}), 162.0 (COO), 123.7, 122.3 (CH), 100.1 (d, J_{C-Rh} = 5.1, CCH_3 Cp*), 72.1 (CHCOO), 38.1 (NCH_3), 9.9 (CH_3 Cp*). MS (ESI+, CH_2Cl_2/MeOH, *m/z*, %): 515.1 ([M-H+Na]$^+$, 100), 493.1 ([M]$^+$, 32). IR (ATR, cm^{-1}): 1738 (COO).

[Cp*IrCl{(MeIm)$_2$CHCOOH}]BF$_4$ (6). HBF$_4 \cdot$OEt$_2$ (9.5 μL, ρ = 1.19 g·mL^{-1}, 0.069 mmol) was added to a solution of [Cp*IrCl{(MeIm)$_2$CHCOO}] (4) (36.7 mg, 0.063 mmol) in CH_2Cl_2 (5 mL). Work up as described above gave the compound as a light yellow solid. Yield: 27.6 mg, 65%. Anal. Calc. for $C_{20}H_{27}BClF_4IrN_4O_2$: C, 35.86; H, 4.06; N, 8.36. Found: C, 35.52; H, 4.09; N, 7.78. ^{1}H NMR (298 K, 300 MHz, CD_2Cl_2): δ 7.57 (d, J_{H-H} = 2.2, 2H, CH), 7.11 (d, J_{H-H} = 2.2, 2H, CH), 5.96 (s, 1H, CHCOO), 4.19 (s, 1H, OH), 3.84 (s, 6H, NCH_3), 1.82 (s, 15H, CH_3 Cp*). $^{13}C\{^1H\}$ NMR (298 K, 75 MHz, CD_2Cl_2): δ 162.5 (COO), 152.6 (C_{NCN}), 123.5, 121.2 (CH), 93.9 (CCH_3 Cp*), 73.3 (CHCOO), 37.8 (NCH_3), 9.8 (CH_3 Cp*). MS (ESI+, CH_2Cl_2/MeOH, *m/z*, %): 583.2 ([M]$^+$, 100). IR (ATR, cm^{-1}): 1738 (COO).

[Cp*RhCl{(MeIm)$_2$CHCOOMe}]OTf (7). CF$_3$SO$_3$Me (16.0 μL, ρ = 1.45 g·mL^{-1}, 0.141 mmol) was added to a solution of [Cp*RhCl{(MeIm)$_2$CHCOO}] (3) (63.1 mg, 0.128 mmol) in CH_2Cl_2 (5 mL). The solution was stirred for 30 minutes at room temperature and then was evaporated to dryness under vacuum to give a light yellow solid. The solid was washed

with cold diethyl ether (3 x 3 mL) and dried under vacuum. Yield: 61.2 mg, 73%. Anal. Calc. for $C_{22}H_{29}ClF_3N_4O_5RhS$: C, 40.22; H, 4.45; N, 8.53; S, 4.88. Found: C, 40.35; H, 4.44; N, 8.49; S, 4.86. ^{1}H NMR (298 K, 300 MHz, CD_2Cl_2): δ 7.42 (d, J_{H-H} = 2.2, 2H, CH), 7.21 (d, J_{H-H} = 2.2, 2H, CH), 6.29 (s, 1H, CHCOO), 4.19 (s, 3H, OCH_3), 3.94 (s, 6H, NCH_3), 1.81 (s, 15H, CH_3 Cp*). $^{13}C\{^1H\}$ NMR (298 K, 75 MHz, CD_2Cl_2): δ 171.4 (d, J_{C-Rh} = 50.9, C_{NCN}), 163.8 (COO), 124.6, 121.5 (CH), 100.7 (d, J_{C-Rh} = 5.4, CCH_3 Cp*), 71.6 (CHCOO), 55.3 (OCH_3), 38.6 (NCH_3), 10.0 (CH_3 Cp*). $^{19}F\{^1H\}$ NMR (298 K, 300 MHz, CD_2Cl_2): δ -79.0 (s, CF$_3$). MS (ESI+, CH_2Cl_2/MeOH, *m/z*, %): 507.2 ([M]$^+$, 100). IR (ATR, cm^{-1}): 1738 (COO). Λ_M = 85.1 $\Omega^{-1} \cdot$cm$^2 \cdot$mol^{-1} (nitromethane).

[Cp*IrCl{(MeIm)$_2$CHCOOMe}]OTf (8). CF$_3$SO$_3$Me (24.4 μL, ρ = 1.45 g·mL^{-1}, 0.216 mmol) and [Cp*IrCl{(MeIm)$_2$CHCOO}] (4) (114.1 mg, 0.196 mmol) were reacted in CH_2Cl_2 (5 mL). Work up as described above gave the compound as a light yellow solid. Yield: 128.6 mg, 88%. Anal. Calc. for $C_{22}H_{29}ClF_3IrN_4O_5S$: C, 35.41; H, 3.92; N, 7.51; 4.30. Found: C, 35.49; H, 3.91; N, 7.45; S, 4.42. ^{1}H NMR (298 K, 300 MHz, CD_2Cl_2): δ 7.33 (d, J_{H-H} = 2.2, 2H, CH), 7.17 (d, J_{H-H} = 2.2, 2H, CH), 6.17 (s, 1H, CHCOO), 4.15 (s, 3H, OCH_3), 3.87 (s, 6H, NCH_3), 1.84 (s, 15H, CH_3 Cp*). $^{13}C\{^1H\}$ NMR (298 K, 75 MHz, CD_2Cl_2): δ 163.8 (COO), 153.7 (C_{NCN}), 124.0, 120.5 (CH), 94.3 (CCH_3 Cp*), 72.2 (CHCOO), 55.3 (OCH_3), 38.0 (NCH_3), 9.8 (CH_3 Cp*). $^{19}F\{^1H\}$ NMR (298 K, 300 MHz, CD_2Cl_2): δ -79.0 (s, CF$_3$). MS (ESI+, CH_2Cl_2/MeOH, *m/z*, %): 597.2 ([M]$^+$, 100). IR (ATR, cm^{-1}): 1761 (COO).

[Cp*Rh(OTf){(MeIm)$_2$CHCOOMe}]OTf (9). CF$_3$SO$_3$Ag (58.9 mg, 0.229 mmol) was added to a solution of [Cp*RhCl{(MeIm)$_2$CHCOOCH$_3$}]OTf (7) (150.5 mg, 0.229 mmol) in CH_2Cl_2 (5 mL) to give a yellow suspension which was stirred for one hour in the absence of light. The suspension was filtered via cannula through Celite and the resulting yellow solution was concentrated to *ca.* 1 mL under reduced pressure. Slow addition of diethyl ether afforded the compound as an intense yellow solid which were filtered, washed with diethyl ether (3 x 3 mL) and dried in vacuo. Yield: 135.0 mg, 76%. Anal. Calc. for $C_{23}H_{29}F_6N_4O_8RhS_2$: C, 35.85; H, 3.79; N, 7.27; S, 8.32. Found: C, 35.80; H, 3.69; N, 6.91; S, 8.13. ^{1}H NMR (298 K, 300 MHz, CD_2Cl_2): δ 7.47 (d, J_{H-H} = 2.2, 2H, CH), 7.29 (d, J_{H-H} = 2.2, 2H, CH), 6.29 (s, 1H, CHCOO), 4.15 (s, 3H, OCH_3), 3.94 (s, 6H, NCH_3), 1.75 (s, 15H, CH_3 Cp*). $^{13}C\{^1H\}$ NMR (298 K, 75 MHz, CD_2Cl_2): δ 169.4 (d, J_{C-Rh} = 52.1, C_{NCN}), 163.7 (COO), 124.7, 122.62 (CH), 102.09 (d, J_{C-Rh} = 6.1, CCH_3 Cp*), 71.76 (CHCOO), 55.3 (OCH_3), 38.9 (NCH_3), 10.3 (CH_3 Cp*). $^{19}F\{^1H\}$ NMR (298 K, 300 MHz, CD_2Cl_2): δ -78.83 (s, Rh-OSO$_2$CF$_3$), -78.91 (s, CF$_3$). HRMS (ESI+, CH_2Cl_2/MeOH, *m/z*, %): 621.1 ([M]$^+$, 100). IR (ATR, cm^{-1}): 1763 (COO). Λ_M = 166.4 $\Omega^{-1} \cdot$cm$^2 \cdot$mol^{-1} (nitromethane).

[Cp*Rh(NCCH$_3$){(MeIm)$_2$CHCOOMe}](OTf)$_2$ (10). [Cp*Rh(OTf){(MeIm)$_2$CHCOOCH$_3$}] OTf (9) (42.5 mg, 0.055 mmol) was dissolved in CH_3CN (3 mL) and stirred for one hour at room temperature to give a pale yellow solution. Concentration of the solution to *ca.* 1 mL and slow diffusion of diethyl ether afforded a microcrystalline shiny yellow powder which was washed with diethyl ether and dried in vacuo. Yield: 29.8 mg, 67 %. Anal. Calc. for $C_{25}H_{32}F_6N_5O_8RhS_2$: C, 36.99; H, 3.97; N, 8.63; S, 7.90. Found: C, 37.18; H, 3.89; N, 8.23; S, 7.85. ^{1}H NMR (298 K, 300 MHz, CD_2Cl_2): δ 7.54 (d, J_{H-H} = 2.2, 2H, CH), 7.39 (d, J_{H-H} = 2.2, 2H, CH), 6.28 (s, 1H, CHCOO), 4.15 (s, 3H, OCH_3), 3.89 (s, 6H, NCH_3), 2.52 (s, 3H, NCCH$_3$), 1.87 (s, 15H, CH_3 Cp*). $^{13}C\{^1H\}$ NMR (298 K, 75 MHz, CD_2Cl_2): δ 166.3 (d, J_{C-Rh} = 49.2, C_{NCN}), 163.4 (COO), 127.7 (d,

J_{C-Rh} = 5.2, NCCH_3) 125.3, 123.1 (CH), 103.1 (d, J_{C-Rh} = 65.7, CCH$_3$ Cp*), 71.7 (CHCOO), 55.4 (OCH_3), 38.6 (NCH_3), 10.2 (CH_3 Cp*), 4.6 (NCCH$_3$). ^{19}F{^{1}H} NMR (298 K, 300 MHz, CD$_2$Cl$_2$): δ -78.92 (s, CF$_3$). HRMS (ESI+, CH$_2$Cl$_2$/CH$_3$CN, m/z, %): 236.0 ([M-CH$_3$CN]$^+$, 7). IR (ATR, cm^{-1}): 1764 (COO). Λ_M = 166.1 $\Omega^{-1} \cdot$cm$^2 \cdot$mol^{-1} (nitromethane).

[Rh(cod){(MeIm)$_2$CHCOO}] (11). _Method A_. [Rh(μ-Cl)(cod)]$_2$ (61.4 mg, 0.124 mmol) was added to a suspension of [(MeImH)$_2$CHCOO]Br (1) (75.0 mg, 0.249 mmol) in THF (10 mL). After 5 minutes of stirring, NaH (21.9 mg, 60% oil dispersion, 0.548 mmol) and MeOH (1 mL) were sequentially added to give an orange solution which was stirred for 4 hours at room temperature. After this time, the solution was brought to dryness under vacuum and the residue extracted with dichloromethane (7 mL) and filtered via cannula to remove inorganic salts. Then, the resulting orange solution was concentrated to _ca._ 1 mL under reduced pressure. Slow addition of acetone afforded a shiny orange solid which was filtered, washed with acetone (3 x 5 mL) and dried in vacuo. Yield: 67.5 mg, 63%. Anal. Calc. for C$_{18}$H$_{23}$N$_4$O$_2$Rh·CH$_3$OH: C 49.36; H, 5.89; N, 12.12. Found: C, 49.48; H, 5.97; N, 11.93. MS (ESI+, CH$_2$Cl$_2$/MeOH, m/z, %): 431.09 ([M+H]$^+$, 100). IR (ATR, cm^{-1}): 1647 (COO). _Method B_. [Rh(μ-OMe)(cod)]$_2$ (60.3 mg, 0.124 mmol) was added to a solution of [(MeImH)$_2$CHCOO]Br (1) (75.0 mg, 0.249 mmol) in THF/MeOH (10 mL, 1:1, (v/v)) to give a yellow suspension which was stirred for 30 min. Then, NaH (10.9 mg, 60% oil dispersion, 0.272 mmol) was added to give immediately a dark orange solution which was stirred for 4 hours at room temperature. After this time, the solution was brought to dryness under vacuum to give an orange residue. Work-up as describe above gave the compound as a shiny orange solid. Yield: 80.4 mg, 75%. Two interconverting isomers, namely _flagpole_ and _bowsprit_, were observed in CD$_2$Cl$_2$ solution in a 3.6/1 ratio. _Flagpole_ isomer (major): ^{1}H NMR (298 K, 400 MHz, CD$_2$Cl$_2$): δ 7.26 (d, J_{H-H} = 2.0, 2H, CH), 6.81 (d, J_{H-H} = 2.1, 2H, CH), 6.03 (s, 1H, CHCOO), 4.84 (m, 4H, =CH cod), 3.73 (s, 6H, NCH$_3$), 2.42 (m, 4H, >CH$_2$ cod), 2.28 (m, 2H, >CH$_2$ cod), 1.91 (m, 2H, >CH$_2$ cod). ^{13}C{^{1}H} NMR (298 K, 101 MHz, CD$_2$Cl$_2$): δ 179.5 (d, J_{C-Rh} = 52.4, C$_{NCN}$), 166.9 (COO), 122.6, 121.5 (CH), 93.9 (d, J_{C-Rh} = 8.4, =CH cod), 86.82 (d, J_{C-Rh} = 8.4, =CH cod), 77.0 (CHCOO), 38.1 (NCH$_3$), 31.2 (>CH$_2$ cod), 30.1 (>CH$_2$ cod). _Bowsprit_ isomer (minor): ^{1}H NMR (298 K, 400 MHz, CD$_2$Cl$_2$): δ 7.95 (d, J_{H-H} = 2.0, 2H, CH), 7.09 (s, 1H, CHCOO), 6.69 (d, J_{H-H} = 2.1, 2H, CH), 4.84 (m, 4H, =CH cod), 3.70 (s, 6H, NCH$_3$), 2.42 (m, 4H, >CH$_2$ cod), 2.28 (m, 2H, >CH$_2$ cod), 1.91 (m, 2H, >CH$_2$ cod). ^{13}C{^{1}H} NMR (298 K, 101 MHz, CD$_2$Cl$_2$): δ 179.5 (d, J_{C-Rh} = 52.4, C$_{NCN}$), 166.9 (COO), 121.9, 120.8 (CH), 91.8 (d, J_{C-Rh} = 8.4, =CH cod), 87.1 (d, J_{C-Rh} = 8.4, =CH cod), 75.7 (CHCOO), 38.0 (NCH$_3$), 31.2 (>CH$_2$ cod), 30.3 (>CH$_2$ cod).

[Rh(nbd){(MeIm)$_2$CHCOO}] (12). The compound was prepared from [(MeImH)$_2$CHCOO]Br (1) (100 mg, 0.332 mmol), [Rh(μ-OMe)(nbd)]$_2$ (75.1 mg, 0.166 mmol) and NaH (14.6 mg, 60% oil dispersion, 0.365 mmol) following the _Method B_ described above and obtained as an orange solid. Yield: 100.4 mg, 73%. Anal. Calc. for C$_{17}$H$_{19}$N$_4$O$_2$Rh: C, 49.29; H, 4.62; N, 13.52. Found: C, 49.18; H, 4.58; N, 13.29. ^{1}H NMR (298 K, 400 MHz, CD$_2$Cl$_2$): δ 7.32 (d, J_{H-H} = 1.7, 2H, CH), 6.78 (d, J_{H-H} = 1.8, 2H, CH), 6.16 (s, 1H, CHCOO), 4.85 (br, 4H, =CH nbd), 3.93 (br, 2H, CH nbd), 3.59 (s, 6H, NCH$_3$), 1.49 (br, 2H, >CH$_2$ nbd). ^{13}C{^{1}H} NMR (298 K, 101 MHz, CD$_2$Cl$_2$): δ 178.8 (d, J_{C-Rh} = 56.2, C$_{NCN}$), 166.7 (COO), 122.0, 121.1 (CH), 79.4 (=CH nbd), 76.6 (CHCOO), 67.5 (>CH$_2$ nbd), 53.9 (CH nbd) 37.4 (NCH$_3$). Both the _flagpole_ and _bowsprit_ isomers in a 5/1 ratio

were observed in CD$_2$Cl$_2$ at 233 K. _Flagpole_ isomer (major): ^{1}H NMR (233 K, 400 MHz, CD$_2$Cl$_2$): δ 7.26 (br, 2H, CH), 6.80 (d, J_{H-H} = 1.6, 2H, CH), 6.11 (s, 1H, CHCOO), 5.00 (m, 2H, =CH nbd), 4.63 (m, 2H, =CH nbd), 3.94 (br, 1H, CH nbd), 3.91 (br, 1H, CH nbd), 3.55 (s, 6H, NCH$_3$), 1.44 (m, 2H, >CH$_2$ cod). ^{13}C{^{1}H} NMR (233 K, 101 MHz, CD$_2$Cl$_2$): δ 177.7 (d, J_{C-Rh} = 55.9, C$_{NCN}$), 167.4 (COO), 121.5, 120.9 (CH), 79.4 (=CH nbd), 75.6 (=CH nbd), 67.3 (>CH$_2$ nbd), 53.8 (CH nbd), 52.3 (CH nbd) 37.2 (NCH$_3$). _Bowsprit_ isomer (minor): ^{1}H NMR (233 K, 400 MHz, CD$_2$Cl$_2$): δ 7.34 (s, 1H, CHCOO), 6.72 (d, J_{H-H} = 1.9, 2H, CH), 6.71 (d, J_{H-H} = 1.9, 2H, CH), 4.02 (br, 2H, CH nbd), 4.00 (br, 1H, CH nbd), 3.32 (m, 2H, =CH nbd), 2.68 (s, 6H, NCH$_3$), 1.76 (m, 2H, >CH$_2$ cod). MS (ESI$^+$, CH$_2$Cl$_2$/MeOH, m/z, %): 446.9 ([M+MeOH]$^+$, 100). IR (ATR, cm^{-1}): 1643 (COO).

[Ir(cod){(MeIm)$_2$CHCOO}] (13). The compound was prepared from [(MeImH)$_2$CHCOO]Br (1) (103.9 mg, 0.345 mmol), [Ir(μ-OMe)(cod)]$_2$ (114.7 mg, 0.173 mmol) and NaH (15.2 mg, 60% oil dispersion, 0.380 mmol) following the _Method B_ described above and obtained as red microcrystalline solid. Yield: 125.5 mg, 70%.[35]

[IrCl(cod){(MeIm)$_2$CHCOO}][IrCl$_2$(cod)] (14). Ag$_2$O (80.4 mg, 0.347 mmol) was added to a solution of [(MeImH)$_2$CHCOO]Br (1) (69.7 mg, 0.231 mmol) in MeOH (5 mL) and the mixture stirred for 16 hours in the absence of light. The suspension was filtered through Celite to give a pale yellow solution which was reacted with [Ir(μ-Cl)(cod)]$_2$ (77.9 mg, 0.116 mmol) for 20 hours in the absence of light. The resulting suspension was filtered off and the solution concentrated under vacuum to _ca._ 1 mL. Slow addition of diethyl ether gave the compound as a yellow solid which was filtered, washed with diethyl ether (3 x 3 mL) and dried in vacuo. Yield: 81.32 mg, 38%. Anal. Calc. for C$_{26}$H$_{35}$Cl$_3$Ir$_2$N$_4$O$_2$: C, 33.71; H, 3.81; N, 6.05. Found: C, 33.56; H, 3.85; N, 5.97. ^{1}H NMR (298 K, 400 MHz, CD$_3$OD): δ 7.77 (d, J_{H-H} = 2.1, 2H, CH), 7.43 (d, J_{H-H} = 2.1, 2H, CH), 6.99 (s, 1H, CHCOO), 6.81 (m, 2H, =CH cod), 5.94 (m, 2H, =CH cod), 4.15 (s, 6H, NCH$_3$), 3.97-3.84 (m, 4H, =CH cod), 2.94-2.79 (m, 4H, >CH$_2$ cod), 2.61-2.49 (m, 2H, >CH$_2$ cod), 2.46-2.33 (m, 2H, >CH$_2$ cod), 2.30-2.09 (m, 4H, >CH$_2$ cod), 1.48-1.31 (m, 4H, >CH$_2$ cod). ^{13}C{^{1}H} NMR (298 K, 101 MHz, CD$_3$OD): δ 166.0 (COO), 135.4 (C$_{NCN}$), 127.4, 122.0 (CH), 117.6, 115.1 (=CH cod), 73.7 (CHCOO), 73.4 (=CH cod), 38.0 (NCH$_3$), 32.7, 30.2, 28.8 (CH$_2$ cod). MS (ESI+, DMSO/MeOH, m/z, %): 555.1 ([M]$^+$, 100). IR (ATR, cm^{-1}): 1694 (COO).

[Rh(cod){(MeIm)$_2$CHCOOMe}]OTf (15). CF$_3$SO$_3$Me (10.3 μL, ρ = 1.45 g·mL^{-1}, 0.091 mmol) was added to a solution of [Rh(cod){(MeIm)$_2$CHCOO}] (11) (39.1 mg, 0.091 mmol) in CH$_2$Cl$_2$ (5 mL). The solution was stirred for 30 minutes and then concentrated under vacuum to _ca._ 1 mL. The slow addition of diethyl ether (2 mL) afforded a dark orange solid which was filtered, washed with diethyl ether (3 x 5 mL) and dried in vacuo. Yield: 40.6 mg, 75%. Anal. Calc. for C$_{20}$H$_{26}$F$_3$N$_4$O$_5$RhS: C, 40.41; H, 4.41; N, 9.43; S, 5.39. Found: C, 40.42; H, 4.41; N, 9.44; S, 5.43. ^{1}H NMR (300 MHz, 298 K, CD$_2$Cl$_2$): δ 7.67 (d, J_{H-H} = 2.0, 2H, CH), 7.29 (s, 1H, CHCOO), 6.87 (d, J_{H-H} = 2.0, 2H, CH), 4.93 (m, 2H, =CH cod), 4.69 (m, 2H, =CH cod), 3.89 (s, 3H, COOCH$_3$), 3.75 (s, 6H, NCH$_3$), 2.59-2.40 (m, 2H, >CH$_2$ cod), 2.32-2.19 (m, 2H, >CH$_2$ cod), 2.11-1.99 (m, 4H, >CH$_2$ cod). ^{13}C{^{1}H} NMR (298 K, 75 MHz, CD$_2$Cl$_2$): δ 180.0 (d, J_{C-Rh} = 52.3 Hz, C$_{NCN}$), 167.0 (COO), 123.4, 122.6 (CH), 93.2 (d, J_{C-Rh} = 8.5 Hz, =CH cod), 89.2 (d, J_{C-Rh} = 7.3 Hz, =CH cod), 72.6 (CHCOO), 54.4 (OCH$_3$), 38.4 (NCH$_3$), 30.9, 30.3 (>CH$_2$ cod). ^{19}F{^{1}H} NMR (300 MHz, 298 K, CD$_2$Cl$_2$): δ -79.0 (s,

CF$_3$). MS (ESI$^+$, CH$_2$Cl$_2$/MeOH, m/z, %): 445.2, ([M]$^+$, 100). IR (ATR, cm^{-1}): 1666 (COO).

[Ir(cod){(MeIm)$_2$CHCOOMe}]OTf (16). CF$_3$SO$_3$Me (7.9 μL, ρ = 1.45 g·mL^{-1}, 0.070 mmol) was added to a solution of [Ir(cod){(MeIm)$_2$CHCOO}] (13) (36.4 mg, 0.070 mmol) in CH$_2$Cl$_2$ (5 mL) at 223 K. The solution was stirred for one hour and allowed to reach room temperature to give a dark red suspension. The suspension was concentrated under vacuum and then filtered to give a dark red solid which was washed with cold diethyl ether (3 x 3 mL) and dried in vacuo. Yield: 32.7 mg, 68%. Anal. Calc. for C$_{20}$H$_{26}$F$_3$IrN$_4$O$_5$S: C, 35.13; H, 3.83; N, 8.19; S, 4.69. Found: C, 34.98; H, 3.75; N, 8.12; S, 4.82. ^{1}H NMR (298 K, 300 MHz, CD$_2$Cl$_2$): δ 7.68 (d, J$_{H-H}$ = 2.0, 2H, CH), 7.15 (s, 1H, CHCOO), 6.97 (d, J$_{H-H}$ = 2.0, 2H, CH), 4.67 (m, 2H, =CH cod), 4.26 (m, 2H, =CH cod), 3.83 (s, 3H, OCH$_3$), 3.75 (s, 6H, NCH$_3$), 2.50-2.31 (m, 2H, >CH$_2$ cod), 2.31-2.13 (m, 2H, >CH$_2$ cod), 2.01-1.68 (m, 4H, >CH$_2$ cod). ^{13}C{^{1}H} NMR (298 K, 75 MHz, CD$_2$Cl$_2$): δ 175.9 (C$_{NCN}$), 166.2 (COO), 122.9 (CH), 81.0, 76.6 (=CH cod), 72.5 (CHCOO), 54.3 (OCH$_3$), 38.3 (NCH$_3$), 31.8, 31.0 (>CH$_2$ cod). ^{19}F{^{1}H} NMR (300 MHz, 298 K, CD$_2$Cl$_2$): δ -79.0 (s, CF$_3$). MS (ESI+, CH$_2$Cl$_2$/MeOH, m/z, %): 535.0 ([M]$^+$, 100). IR (ATR, cm^{-1}): 1658 (COO).

Reaction of [Rh(cod){(MeIm)$_2$CHCOO}] (11) with HBF$_4$·OEt$_2$. HBF$_4$·OEt$_2$ (2.99 μL, ρ = 1.19 g·mL^{-1}, 0.022 mmol) was added to a solution of [Rh(cod){(MeIm)$_2$CHCOO}] (11) (10.0 mg, 0.022 mmol) in CH$_2$Cl$_2$ (5 mL). The solution was stirred for 30 minutes at room temperature and then was brought to dryness under vacuum. The orange solid was washed with diethyl ether (3 x 3 mL) and dried in vacuo. The ^{1}H NMR spectra of this solid revealed the formation of complex [Rh(cod){(MeIm)$_2$CH$_2$}]BF$_4$ (17).[58] Yield: 9.60 mg, 92%.

Reaction of [Ir(cod){(MeIm)$_2$CHCOO}] with HBF$_4$·OEt$_2$. HBF$_4$·Et$_2$O (7.7 μL, ρ = 1.19 g·mL^{-1}, 0.056 mmol) was added to a red suspension of [Ir(cod){(MeIm)$_2$CHCOO}] (22) (29.1 mg, 0.056 mmol) in CH$_2$Cl$_2$ (3 mL) at 223 K. The colour of the suspension progressively changed to yellow. After 10 minutes of stirring at this temperature the solvent was removed under vacuum and the yellow solid washed with diethyl ether (3 x 3 mL) and dried in vacuo. The ^{1}H NMR spectra of this solid revealed the formation of the hydrido iridium(III) complex [IrH(cod){(MeIm)$_2$CHCOO}]BF$_4$ (18) which has been characterized by comparison of the spectroscopic properties with those of the triflate salt.[35] Yield: 24.5 mg, 72%.

[Ir(CH$_3$)(cod){(MeIm)$_2$CHCOO}]I (19). A dark red suspension of [Ir(cod){(MeIm)$_2$CHCOO}] (13) (27.0 mg, 0.052 mmol) in CH$_3$I (2 mL) was stirred for 30 min to give a yellow suspension. The solvent was removed under vacuum to give a yellow solid which was washed with diethyl ether (3 x 3 mL) and dried in vacuo. Yield: 27.1 mg, 79%. Anal. Calc. for C$_{19}$H$_{26}$IIrN$_4$O$_2$: C, 34.50; H, 3.96; N, 8.47. Found: C, 34.41; H, 3.90; N, 8.53. ^{1}H NMR (298 K, 300 MHz, CD$_3$OD): δ 7.71 (d, J$_{H-H}$ = 2.1, 2H, CH), 7.33 (d, J$_{H-H}$ = 2.1, 2H, CH), 6.83 (s, 1H, CHCOO), 6.03 (m, 2H, =CH cod), 5.22 (m, 2H, =CH cod), 3.92 (s, 6H, NCH$_3$), 2.77-2.68 (m, 2H, >CH$_2$ cod), 2.68-2.60 (m, 2H, >CH$_2$ cod), 2.60-2.51 (m, 2H, >CH$_2$ cod), 2.27-2.17 (m, 2H, >CH$_2$ cod), 1.58 (s, 3H, Ir-CH$_3$). ^{13}C{^{1}H} NMR (298 K, 75 MHz, CD$_3$OD): δ 168.0 (COO), 147.3 (C$_{NCN}$), 127.0, 121.6 (CH), 105.6, 105.1 (CH cod), 75.0 (CHCOO), 38.1 (NCH$_3$), 30.1, 29.0 (>CH$_2$ cod), -29.5 (Ir-CH$_3$). MS (ESI+, MeOH, m/z, %): 535.0 ([M]$^+$, 100). IR (ATR, cm^{-1}): 1662 (COO). Λ$_M$ = 83.2 Ω^{-1}·cm^2·mol^{-1} (methanol).

Synthesis of [IrI(cod){(MeIm)$_2$CHCOO}]I (20). Solid I$_2$ (7.61 mg, 0.030 mmol) was added to a solution of [Ir(cod){(MeIm)$_2$CHCOO}] (13) (15.6 mg, 0.030 mmol) in MeOH (5 mL) to give a dark yellow solution after stirring for 10 minutes. The solvent was removed under vacuum and the resulting yellow solid was washed with diethyl ether (3 x 3 mL) and dried in vacuo. Yield: 20.2 mg, 87%. Anal. Calc. for C$_{18}$H$_{23}$I$_2$IrN$_4$O$_2$: C, 27.95; H, 3.00; N, 7.24. Found: C, 28.09; H, 3.11; N, 7.18. ^{1}H NMR (298 K, 300 MHz, CD$_3$OD): δ 7.76 (d, J$_{H-H}$ = 2.0, 2H, CH), 7.47 (d, J$_{H-H}$ = 2.0, 2H, CH), 7.01 (s, 1H, CHCOO), 6.96 (m, 2H, =CH cod), 5.68 (m, 2H, =CH cod), 4.15 (s, 6H, NCH$_3$), 3.17-3.09 (m, 4H, >CH$_2$ cod), 2.64-2.53 (m, 2H, >CH$_2$ cod), 2.45-2.33 (m, 2H, >CH$_2$ cod). ^{13}C{^{1}H} NMR (298 K, 75 MHz, CD$_3$OD): δ 165.9 (COO), 134.3 (C$_{NCN}$), 127.6, 122.1 (CH), 111.7, 110.6 (=CH cod), 73.7 (CHCOO), 40.0 (NCH$_3$), 32.9, 28.3 (>CH$_2$ cod). MS (ESI+, MeOH, m/z, %): 647.0 ([M]$^+$, 100). IR (ATR, cm^{-1}): 1662 (COO). Λ$_M$ = 84.7 Ω^{-1}·cm^2·mol^{-1} (methanol).

Determination of the kinetic parameters by 2D-EXSY NMR spectroscopy. The kinetic parameters for the equilibrium between the *flagpole* and *bowsprit* isomers in zwitterionic complex [Rh(cod){(MeIm)$_2$CHCOO}] (11) were obtained from the ^{1}H 2D-EXSY NMR spectra (300.13 MHz) by using a gradient-selected NOESY program from Bruker (noesygpph pulse sequence). 2D-EXSY NMR spectra (300 MHz) were recorded using a concentrated solution of 11 in CD2Cl2 with an optimized mixing time of 284 ms. The integrations for the exchange cross-peaks between the well separated =CH imidazole-2-carbene proton resonances from the rest in the NMR spectrum for both isomers were processed using the EXSYCalc program to compute the rate constants k_1 and k_{-1} (s^{-1}), K_{EXSY}: calculated equilibrium constant from EXSY determined rate constants (k$_1$/k$_{-1}$).[67] K_{Int}: experimental equilibrium constant obtained from the integration of the methyl resonances of both isomers in the ^{1}H NMR spectrum. The activation barriers for the forward and reverse processes were derived from the Eyring equation.[50]

Computational Details. DFT calculations performed in this work were carried out with the Gaussian09 program (revision D.01).[68] The calculations for geometry optimization and relative stability of the stereoisomers of [Cp*RhCl{(MeIm)$_2$CHCOO}] (3), [Cp*RhX{(MeIm)$_2$CHCOOMe}]OTf (X = Cl, 7; OTf, 9) and [M(diene){(MeIm)-CHCOO}] (M = Rh, diene = cod, 11, nbd, 12; Ir, cod, 13) were performed using the B3LYPfunctional,[69,70,71] including Grimme D3 dispersion[72] correction with Becke-Johnson type damping and solvent correction using the PCM approach for methanol and dichloromethane.[73] For Rh atoms the LANL2DZ and its associated basis set supplemented with an f function was used.[74] The 6-31G(d,p) basis set was used for the rest of the atoms.

Crystal structure determinations. Single crystals for the X–ray diffraction studies were grown by: i) slow evaporation of a concentrated methanol solution of 1, ii) slow diffusion of diethyl ether into a concentrated dichloromethane/MeOH solution of 3 or 4, iii) slow evaporation of a concentrated dichloromethane solution of 8 or 9, iv) cooling a concentrated methanolic solution of 11 or 12, and v) slow diffusion of diethyl ether into a concentrated dichloromethane solution of 14. X–ray diffraction, data were collected on APEX SMART or APEX–DUO SMART Bruker diffractometers with graphite–monochromated Mo–Kα radiation (λ = 0.71073 Å) using narrow ω rotations (0.3–0.6°). Intensities were integrated and corrected for absorption effects with SAINT-PLUS,[75] and SADABS[76] programs, both included in APEX2 package. The

structures were solved by the Patterson method with SHELXS-2013[77] and refined by full matrix least–squares on F^2 with SHELXL-2014[78] under WinGX.[79] The analysis of the interatomic contacts was performed with PARST.[80]

Crystal data for **1**·3H$_2$O. $C_{10}H_{19}BrN_4O_5$, M = 355.20 g mol^{-1}, T = 100(2) K, orthorhombic, Pnma, a = 5.9080(5) Å, b = 12.0155(11) Å, c = 21.615(2) Å, V = 1534.4(2) Å^3, Z = 4, D_c = 1.538 Mg m^{-3}, μ = 2.703 mm^{-1}, colorless needle, 0.300 x 0.100 x 0.080 mm^3, ∨$_{min}$/∨$_{max}$ 1.884/26.365°, reflections collected/unique 10102/1642 [R(int) = 0.0527], data/restraints/parameters 1642/7/124, GoF = 1.052, R_1 = 0.0407 [I>2∨(I)], wR$_2$ = 0.1015 (all data), largest diff. peak/hole 0.830/−0.643 e Å^{-3}.

Crystal data for **3**·CH$_3$OH. $C_{21}H_{30}ClN_4O_3Rh$, M = 524.85 g mol^{-1}, T = 100(2) K, monoclinic, P2$_1$/m, a = 7.1476(5) Å, b = 11.2375(9) Å, c = 13.3953(10) Å, β = 97.1260(10)°, V = 1067.62(14) Å^3, Z = 2, D_c = 1.633 Mg m^{-3}, μ = 0.956 mm^{-1}, yellow prism, 0.240 x 0.130 x 0.040 mm^3, ∨$_{min}$/∨$_{max}$ 1.532/26.366°, reflections collected/unique 14384/2290 [R(int) = 0.0349], data/restraints/parameters 2290/0/158, GoF = 1.102, R_1 = 0.0254 [I>2∨(I)], wR$_2$ = 0.0561 (all data), largest diff. peak/hole 0.554/−0.447 e Å^{-3}.

Crystal data for **4**·CH$_3$OH. $C_{21}H_{30}ClIrN_4O_3$, M = 614.14 g mol^{-1}, T = 100(2) K, monoclinic, P2$_1$/m, a = 7.1866(5) Å, b = 11.2275(8) Å, c = 13.3880(9) Å, β = 96.9610(10)°, V = 1072.28(13) Å^3, Z = 2, D_c = 1.902 Mg m^{-3}, μ = 6.382 mm^{-1}, yellow prism, 0.130 x 0.110 x 0.100 mm^3, ∨$_{min}$/∨$_{max}$ 2.375/26.368°, reflections collected/unique 8682/2287 [R(int) = 0.0281], data/restraints/parameters 2287/0/156, GoF = 1.113, R_1 = 0.0222 [I>2∨(I)], wR$_2$ = 0.0540 (all data), largest diff. peak/hole 1.380/−0.712 e Å^{-3}.

Crystal data for **8**. $C_{22}H_{29}ClF_3IrN_4O_5S$, M = 746.20 g mol^{-1}, T = 150(2) K, orthorhombic, Pbca, a = 20.420(3) Å, b = 12.697(2) Å, c = 20.851(4) Å, V = 5405.9(16) Å^3, Z = 8, D_c = 1.834 Mg m^{-3}, μ = 5.176 mm^{-1}, orange prism, 0.210 x 0.120 x 0.100 mm^3, ∨$_{min}$/∨$_{max}$ 1.953/26.372°, reflections collected/unique 86429/5523 [R(int) = 0.0430], data/restraints/parameters 5523/0/342, GoF = 1.054, R_1 = 0.0193 [I>2∨(I)], wR$_2$ = 0.0447 (all data), largest diff. peak/hole 0.883/−0.353 e Å^{-3}.

Crystal data for **9**. $C_{23}H_{29}F_6N_4O_8RhS_2$, M = 770.53 g mol^{-1}, T = 100(2) K, triclinic, P−1, a = 8.3758(12) Å, b = 12.9661(19) Å, c = 14.650(2) Å, α = 77.797(2)°, β = 75.637(2)°, γ = 89.215(2)°, V = 1505.2(4) Å^3, Z = 2, D_c = 1.700 Mg m−3, μ = 0.795 mm^{-1}, orange prism, 0.090 x 0.080 x 0.030 mm^3, ∨$_{min}$/∨$_{max}$ 1.931/26.371°, reflections collected/unique 15236/6112 [R(int) = 0.0618], data/restraints/parameters 6112/0/405, GoF = 0.988, R_1 = 0.0417 [I>2∨(I)], wR$_2$ = 0.0864 (all data), largest diff. peak/hole 0.641/−0.727 e Å^{-3}.

Crystal data for **11**·2CH$_3$OH. $C_{20}H_{31}N_4O_4Rh$, M = 494.40 g mol^{-1}, T = 100(2) K, Monoclinic P2$_1$/n, a = 10.3943(12) Å, b = 14.5558(16) Å, c = 14.2031(16) Å, β = 98.651(2)°, V = 2124.4(4) Å^3, Z = 4, D_c = 1.546 Mg m^{-3}, μ = 0.837 mm^{-1}, orange prism, 0.20 x 0.16 x 0.13 mm^3, ∨$_{min}$/∨$_{max}$ 2.02/26.373°, reflections collected/unique 14978/4246 [R(int) = 0.0276], data/restraints/parameters 4246/0/268, GoF = 1.037, R_1 = 0.0285 [I>2∨(I)], wR$_2$ = 0.0770 (all data), largest diff. peak/hole 0.926/−0.590 e Å^{-3}.

Crystal data for **12**·2CH$_3$OH. $C_{19}H_{25}N_4O_4Rh$, M = 476.34 g mol^{-1}, T = 100(2) K, orthorhombic, Pnma, a = 7.9662(10) Å, b = 18.344(2) Å, c = 13.6932(17) Å, V = 2001.0(4) Å^3, Z = 4, D_c = 1.581 Mg m^{-3}, μ = 0.886 mm^{-1}, orange prism, 0.250 x 0.250 x 0.240 mm^3, ∨$_{min}$/∨$_{max}$ 1.856/26.351°, reflections collected/unique 26971/2105 [R(int) = 0.0241],

data/restraints/parameters 2105/0/139, GoF = 1.064, R_1 = 0.0201 [I>2∨(I)], wR$_2$ = 0.0530 (all data), largest diff. peak/hole 0.552/−0.326 e Å^{-3}.

Crystal data for **14**. $C_{26}H_{35}Cl_3Ir_2N_4O_2$, M = 926.33 g mol^{-1}, T = 100(2) K, Triclinic P−1, a = 8.230(2) Å, b = 12.545 (4) Å, c = 13.129(4) Å α = 87.246(4), β = 86.263(3), γ = 82.917(3)°, V = 1341.3(6) Å^3, Z = 2, D_c = 2.294 Mg m^{-3}, μ = 10.244 mm^{-1}, yellow prism, 0.160 x 0.130 x 0.080 mm^3, ∨$_{min}$/∨$_{max}$ 1.556/26.372°, reflections collected/unique 14370/5451 [R(int) = 0.0235], data/restraints/parameters 5451/0/336 GoF = 1.087, R_1 = 0.0293 [I>2∨(I)], wR$_2$ = 0.0694 (all data), largest diff. peak/hole 1.294/−1.984 e Å^{-3}.

ASSOCIATED CONTENT

Supporting Information Available. The Supporting Information is available free of charge on the ACS Publications website at DOI: 10.1021/acs.inorgchem.XXXX. NMR spectra for selected compounds, experimental procedure for the determination of the kinetic parameters by 2D-EXSY spectroscopy and determination of the thermodynamic parameters for the isomerization equilibrium (PDF). Electronic energy, enthalpy, and free energy and optimized coordinates for the computed compounds (XYZ).

Accession Codes

CCDC #1824381 (**1**), #1824382 (**3**), #1824383 (**4**), #1824384 (**8**), #1824385 (**9**), #1824386 (**11**), #1824387 (**12**) and #1824388 (**14**) contain the supplementary crystallographic data for this paper. These data can be obtained free of charge via www.ccdc.cam.ac.uk/data_request/cif, or by emailing data_request@ccdc.cam.ac.uk, or by contacting The Cambridge Crystallographic Data Centre, 12 Union Road, Cambridge CB2 1EZ, UK; fax: +44 1223 336033.

AUTHOR INFORMATION

Corresponding Author

* E-mail for J.J.P-T.: perez@unizar.es. E-mail for M.V.J.: vjimenez@unizar.es

ORCID
M. Victoria Jiménez: 0000-0002-0545-9107
Fernando Lahoz: 0000-0001-8054-2237
Javier Modrego: 0000-0002-9633-3285
Vincenzo Passarelli: 0000-0002-1735-6439
Jesús J. Pérez-Torrente: 0000-0002-3327-0918

Notes

The authors declare no competing financial interest.

ACKNOWLEDGMENTS

REFERENCES

[1] *N-Heterocyclic Carbenes*; Diez-Gonzalez, S., Ed; Catalysis Series; The Royal Society of Chemistry, **2017**.

[2] Hopkinson, M. N.; Richter, C.; Schedler, M.; Glorius, F. An overview of N-heterocyclic carbenes. Nature **2014**, 510, 485–496.

[3] Mercs, L.; Albrecht, M. Beyond catalysis: N-heterocyclic carbene complexes as components for medicinal, luminescent, and functional materials applications. *Chem. Soc. Rev.* **2010**, *39*, 1903–1912.

[4] Charra, V.; de Frémont, P.; Braunstein, P. Multidentate N-heterocyclic carbene complexes of the 3d metals: Synthesis, structure, reactivity and catalysis. *Coord. Chem. Rev.* **2017**, *341*, 53–176.

[5] Biffis, A.; Baron, M.; Tubaro, C. Poly-NHC Complexes of Transition Metals: Recent Applications and New Trends. In *Adv. in Organomet. Chem.*; Pérez, P. J., Ed.; Academic Press, **2015**; Vol. 63, cap. 5, pp 203–288.

[6] Pugh, D.; Danopoulos, A. A. Metal complexes with 'pincer'-type ligands incorporating N-heterocyclic carbene functionalities. *Coord. Chem. Rev.* **2007**, *251*, 610–641.

[7] Blanco, M.; Álvarez, P.; Blanco, C.; Jiménez, M. V.; Fernández-Tornos, J.; Pérez-Torrente, J. J.; Oro, L. A.; Menéndez, R. Enhanced Hydrogen-Transfer Catalytic Activity of Iridium N-Heterocyclic Carbenes by Covalent Attachment on Carbon Nanotubes, *ACS Catal.* **2013**, 3, 1307–1317.

[8] Santini, C.; Marinelli, M.; Pellei, M. Boron-Centered Scorpionate-Type NHC-Based Ligands and Their Metal Complexes. *Eur. J. Inorg. Chem.* **2016**, 2312–2331.

[9] Sinha, N.; Tan, T. T. Y.; Peris, E.; Hahn, F. E. High-Fidelity, Narcissistic Self-Sorting in the Synthesis of Organometallic Assemblies from Poly-NHC Ligands. *Angew. Chem. Int. Ed.* **2017**, *56*, 7393–7397.

[10] Poyatos, M.; Mata, J. A.; Peris, E. Complexes with poly(N-heterocyclic carbene) ligands: Structural features and catalytic applications. *Chem. Rev.* **2009**, *109*, 3677–3707.

[11] Leung, C. H.; Incarvito, C. D.; Crabtree, R. H. Interplay of Linker, N-Substituent, and Counterion Effects in the Formation and Geometrical Distortion of N-Heterocyclic Biscarbene Complexes of Rhodium(I). *Organometallics* **2006**, *25*, 6099–6107.

[12] Straubinger, C. S.; Jokić, N. B.; Högerl, M. P.; Herdtweck, E.; Herrmann, W. A.; Kühn, F. E. Bridge functionalized bis-N-heterocyclic carbene rhodium(I) complexes and their application in catalytic hydrosilylation. *J. Organomet. Chem.* **2011**, *696*, 687–692.

[13] Andrew, R. E.; González-Sebastián, L. Chaplin A. B. NHC-based pincer ligands: carbenes with a bite. *Dalton Trans.*, **2016**, *45*, 1299–1305.

[14] Filonenko, G. A.; Aguila, M. J. B.; Schulpen, E. N.; van Putten, R.; Wiecko, J.; Mueller, C.; Lefort, L.; Hensen, E. J. M.; Pidko, E. A. Bis-N-heterocyclic Carbene Aminopincer Ligands Enable High Activity in Ru-Catalyzed Ester Hydrogenation. *J. Am. Chem. Soc.* **2015**, *137*, 7620–7623.

[15] Arnold, P. L.; Scarisbrick, A. C. Di- and Trivalent Ruthenium Complexes of Chelating, Anionic N-Heterocyclic Carbenes. *Organometallics* **2004**, *23*, 2519–2521.

[16] Mas-Marzá, E.; Poyatos, M.; Sanaú, M.; Peris, E. A new rhodium(III) complex with a tripodal bis(imidazolylidene) ligand. Synthesis and catalytic properties. Organometallics **2004**, 23, 323–325.

[17] Sinha, N.; Roelfes, F.; Hepp, A.; Hahn, F. E. Single-Step Synthesis of Organometallic Molecular Squares from *NR,NR',NR'',NR'''*-Substituted Benzobiscarbenes. *Chem. Eur. J.* **2017**, *23*, 5939–5942.

[18] Sabater, S.; Mata, J. A.; Peris, E. Hydrodefluorination of carbon–fluorine bonds by the synergistic action of a ruthenium–palladium catalyst. *Nature Commun.* **2013**, *4*, 3553–3560.

[19] A. Nasr, A. Winkler, M. Tamm, Anionic N-heterocyclic carbenes: Synthesis, coordination chemistry and applications in homogeneous catalysis. *Coord. Chem. Rev.* **2016**, *316*, 68–124.

[20] Stradiotto, M.; Hesp, K. D.; Lundgren, R. J. Zwitterionic Relatives of Cationic Platinum Group Metal Complexes: Applications in Stoichiometric and Catalytic σ-Bond Activation. *Angew. Chem. Int. Ed.* **2010**, *49*, 494–512.

[21] Kolychev, E. L.; Kronig, S.; Brandhorst, K.; Freytag, M.; Jones, P. G.; Tamm, M. Iridium(I) Complexes with Anionic N-Heterocyclic Carbene Ligands as Catalysts for the Hydrogenation of Alkenes in Nonpolar Media. *J. Am. Chem. Soc.*, **2013**, *135*, 12448–12459.

[22] Viciano, M.; Mas-Marzá, E.; Poyatos, M.; Sanaú, M.; Crabtree, R. H.; Peris, E. An N-heterocyclic carbene/iridium hydride complex from the oxidative addition of a ferrocenyl-bisimidazolium salt: Implications for synthesis. *Angew. Chem. Int. Ed.* **2005**, *44*, 444–447.

[23] Mas-Marzá, E.; Sanaú, M.; Peris, E. A new pyridine-bis-N-heterocyclic carbene ligand and its coordination to Rh: Synthesis and characterization. *J. Organomet. Chem.* **2005**, *690*, 5576–5580.

[24] Kühl, O. US2013171071 (A1), **2013**.

[25] Díez-Barra, E.; Guerra, J.; Hornillos, V.; Merino, S.; Tejeda, J. Double Michael addition of azoles to methyl propiolate: a straightforward entry to ligands with two heterocyclic rings. *Tetrahedron Lett.* **2004**, *45*, 6937-6939.

[26] Díez-Barra, E.; Guerra, J.; Hornillos, V.; Merino, S.; Tejeda, J. Synthesis of palladium–biscarbene complexes derived from 1,10-methylenebis(1,2,4-triazole) functionalized in the methylene bridge. *J. Organomet. Chem.* **2005**, *690*, 5654–5661.

[27] Rieb, J.; Dominelli, B.; Mayer, D.; Jandl, C.; Drechsel, J.; Heydenreuter, W.; Sieber, S. A.; Kühn, F. E. Influence of wing-tip substituents and reaction conditions on the structure, properties and cytotoxicity of Ag(I) and Au(I)–bis(NHC) complexes. *Dalton Trans.* **2017**, *46*, 2722–2735.

[28] Zhong, R.; Pöthig, A.; Mayer, D. C.; Jandl, C.; Altmann, P. J.; Herrmann, W. A.; Kühn, F. E. Spectroscopic and Structural Properties of Bridge-Functionalized Dinuclear Coinage-Metal (Cu, Ag, and Au) NHC Complexes: A Comparative Study. *Organometallics* **2015**, *34*, 2573–2579.

[29] Zhong, R.; Pöthig, A.; Haslinger, S.; Hofmann, B.; Raudaschl-Sieber, G.; Herdtweck, E.; Herrmann, W. A.; Kühn, F. E. Toward Tunable Immobilized Molecular Catalysts: Functionalizing the Methylene Bridge of Bis(N-heterocyclic carbene) Ligands. *ChemPlusChem* **2014**, *79*, 1294–1303.

[30] Desai, S. P.; Mondal, M.; Choudhury, J. Chelating Bis-N-heterocyclic Carbene–Palladium(II) Complexes for Oxidative Arene C–H Functionalization. *Organometallics* **2015**, *34*, 2731–2736.

[31] Fareghi-Alamdari, R.; Saeedi, M. S.; Panahi, F. New bis(N-heterocyclic carbene) palladium complex immobilized on magnetic nanoparticles: as a magnetic reusable catalyst in Suzuki-Miyaura cross coupling reaction. *Appl. Organomet. Chem.* **2017**, *31*, e3870.

[32] Mata, J. A.; Poyatos, M.; Peris, E. Structural and catalytic properties of chelating bis- and tris-N-heterocyclic carbenes. *Coord. Chem. Rev.* **2007**, *251*, 841–859.

[33] Jiménez, M. V.; Fernández-Tornos, J.; Pérez-Torrente, J. J.; Modrego, F. J.; Winterle, S.; Cunchillos, C.; Lahoz, F. J.; Oro, L. A. Iridium(I) complexes with hemilabile N-heterocyclic carbenes: Efficient and versatile transfer hydrogenation catalysts. *Organometallics* **2011**, *30*, 5493–5508.

[34] Jiménez, M. V.; Pérez-Torrente, J. J.; Bartolomé, M. I.; Gierz, V.; Lahoz, F. J.; Oro, L. A. Rhodium(I) complexes with hemilabile N-heterocyclic carbenes: Efficient alkyne hydrosilylation catalysts . *Organometallics* **2008**, *27*, 224–234.

[35] Puerta-Oteo, R.; Hölscher, M.; Jiménez, M. V.; Leitner, W.; Passarelli, V.; Pérez-Torrente, J. J. Experimental and Theoretical Mechanistic Investigation on the Catalytic CO₂ Hydrogenation to Formate by a Carboxylate-Functionalized Bis(*N*-heterocyclic

carbene) Zwitterionic Iridium(I) Compound. *Organometallics* **2017**, 10.1021/acs.organomet.7b00509.

[36] Ahrens, S.; Strassner, T. Detour-free synthesis of platinum-bis-NHC chloride complexes, their structure and catalytic activity in the CH activation of methane. *Inorg. Chim. Acta* **2006**, *359*, 4789–4796.

[37] Leclercq, L.; Noujeim, N.; Schmitzer, A. R. Development of N,N'-Diaromatic Diimidazolium Cations: Arene Interactions for Highly Organized Crystalline Materials. *Cryst. Growth Des.* **2009**, *9*, 4784–4792.

[38] For the sake of comparison, gas-phase bond lengths in acetic acid and trifluoroacetic acid are C=O 1.214 Å, C–O 1.364 Å and C=O 1.192 Å, C–O 1.35 Å, respectively (see CRC Handbook of Chemistry and Physics, 99th edition, 2018, CRC Press, ISBN 978-1138561632.

[39] Quezada, C. A.; Garrison, J. C.; Panzner, M. J.; Tessier, C. A.; Youngs, W. J. The Potential Use of Rhodium N-Heterocyclic Carbene Complexes as Radiopharmaceuticals: The Transfer of a Carbene from Ag(I) to $RhCl_3 \cdot 3H_2O$. *Organometallics* **2004**, *23*, 4846–4848.

[40] J. Garrison, C.; Youngs, W. J. Ag(I) N-Heterocyclic Carbene Complexes: Synthesis, Structure, and Application. *Chem. Rev.* **2005**, *105*, 3978–4008.

[41] Haque, R. A.; Budagumpi, S.; Zetty Zulikha, H.; Hasanudin, N.; Khadeer Ahamed, M. B.; Abdul Majid, A. M. S. Silver(I)-N-heterocyclic carbene complexes of nitrile-functionalized imidazol-2-ylidene ligands as anticancer agents. *Inorg. Chem. Commun.* **2014**, *44*, 128–133.

[42] Moss, G. P. Basic Terminology of Stereochemistry. *Pure Appl. Chem.* **1996**, *68*, 2193-2222.

[43] Azpíroz, R.; Rubio-Pérez, L.; Di Giuseppe, A.; Passarelli, V.; Lahoz, F. J.; Castarlenas, R.; Pérez-Torrente, J. J. Oro, L. A. Rhodium(I)-N-Heterocyclic Carbene Catalyst for Selective Coupling of *N*-Vinylpyrazoles with Alkynes via C–H Activation. *ACS Catal.* **2014**, *4*, 4244–4253.

[44] Cremer and Pople puckering paramenters of the six member ring Rh-C(1)-N(5)-C(7)-N(9)-C(10) in **8** and **9** are: **8**, q_2 = 0.7961(0.0023), q_3 = −0.0270(0.0021), θ_2 = −175.60(0.18); QT 0.7965(0.0023); ψ_2 = 91.94(0.15); **9**, q_2 = 0.5823(0.0034), q_3 = −0.0210(0.0034), θ_2 = −177.24(0.31), QT = 0.5827(0.0034), ψ_2 = 92.06(0.34) (see Cremer, D.; Pople J. A. *J. Am. Chem. Soc.* **1975**, *97*, 1354–1358).

[45] Scherer, W.; Dunbar, A. C.; Barquera-Lozada, J. E.; Schmitz, D.; Eickerling, G.; Kratzert, D.; Stalke, D.; Lanza, A.; Macchi, P.; Casati, N. P. M.; Ebad-Allah, J.; Kuntscher, C. Anagostic Interactions under Pressure: Attractive or Repulsive? *Angew. Chem. Int. Ed.* **2015**, *54*, 2505–2509.

[46] Huynh, H. V.; Wong, L. R.; Ng, P. S. Anagostic Interactions and Catalytic Activities of Sterically Bulky Benzannulated N-Heterocyclic Carbene Complexes of Nickel(II). *Organometallics* **2008**, *27*, 2231–2237.

[47] Brookhart, M.; Green, M. L. H.; Parkin, G. Agostic interactions in transition metal compounds. *Proc. Natl. Acad. Sci.* **2007**, *104*, 6908–6914.

[48] Nikitin, K.; Bothe, C.; Müller-Bunz, H.; Ortin, Y.; McGlinchey, M. J. High and Low Rotational Barriers in Metal Tricarbonyl Complexes of 2- and 3-Indenyl Anthracenes and Triptycenes: Rational Design of Molecular Brakes. *Organometallics* **2012**, *31*, 6183–6198.

[49] Bertrand, G.; Díez-Barra, E.; Fernández-Baeza, J.; Gornitzka, H.; Moreno, A.; Otero, A.; Rodríguez-Curiel, R. I.; Tejeda J. Synthesis, Characterization and Dynamic Behavior of Mono- and Dinuclear Palladium(II) Carbene Complexes Derived From 1,1'-Methylenebis(4-alkyl-1,2,4-triazolium) Diiodides. *Eur. J. Inorg. Chem.* **1999**, 1965–1971.

[50] Atkins, P. W.; De Paula, J. In *Atkins' Physical chemistry*, Oxford University Press: Oxford, **2010**.

[51] Hornillos, V.; Guerra, J.; de Cózar, A.; Prieto, P.; Merino, S.; Maestro, M. A.; Díez-Barra, E.; Tejeda, J. Synthesis and characterization of metallodendritic palladium-biscarbene complexes derived from 1,1'-methylenebis(1,2,4-triazole). *Dalton Trans.* **2011**, *40*, 4095–4103.

[52] Canty, A. J.; Hoare, J. L.; W. Skelton, B.; White, A. H.; van Koten, G. Synthesis and reactivity of poly(pyrazol-1-yl)borate derivatives of cyclopalladation systems, including structural studies of $Pd\{2\text{-}CH_2C_6H_4P(o\text{-tolyl})_2\text{-C,P}\}\{(pz)_3BH\text{-N,N}'\}$ and $Pd(C_6H_4C_5H_4N\text{-C2,N}')\{(pz)_3BH\text{-N,N}'\}$. *J. Organomet. Chem.* **1998**, *552*, 23–29.

[53] Gott, A. L.; McGowan, P. C.; Temple, C. N. Controlling the Coordination Mode of 1,4,7-Triazacyclononane Complexes of Rhodium and Iridium and Evaluating Their Behavior as Phenylacetylene Polymerization Catalysts. *Organometallics* **2008**, *27*, 2852–2860.

[54] Riener, K.; Zimmermann, T. K.; Pothig, A.; Herrmann, W. A.; Kuhn F. E. Direct Synthesis and Bonding Properties of the First $\mu^2\text{-}\eta^2,\eta^2$-Allyl-Bridged Diiridium Complex. *Inorg. Chem.* **2015**, *54*, 4600–4602.

[55] Arumugam, K.; Chang, J.; Lynch, V. M.; Bielawski, C. W. Cationic Iridium Complexes Containing Anionic Iridium Counterions Supported by Redox-Active N-Heterocyclic Carbenes. *Organometallics* **2013**, *32*, 4334–4341.

[56] Aliaga-Lavrijsen, M.; Iglesias, M.; Cebollada, A.; Garcés, K.; García, N.; Sanz Miguel, P. J.; Fernández-Alvarez, F. J.; Pérez-Torrente, J. J.; Oro, L. A. Hydrolysis and Methanolysis of Silanes Catalyzed by Iridium(III) Bis-N-Heterocyclic Carbene Complexes: Influence of the Wingtip Groups. *Organometallics* **2015**, *34*, 2378.

[57] Azua, A.; Sanz, S.; Peris, E. Water-soluble Ir^{III}-*N*-heterocyclic carbene based catalysts for the reduction of CO2 to formate by transfer hydrogenation and the deuteration of aryl amines in water. *Chem. Eur. J.* **2011**, *17*, 3963.

[58] Frey, G. D.; Rentzsch, C. F.; von Preysing, D.; Scherg, T.; Mühlhofer, M.; Herdtweck, E.; Herrmann, W. A. Rhodium and iridium complexes of N-heterocyclic carbenes: Structural investigations and their catalytic properties in the borylation reaction. *J. Organomet. Chem.* **2006**, *691*, 5725–5738.

[59] Golden, M.; Darensbourg, M.; Irwin, J.; Frost, B. In *Inorganic Syntheses: Volume 36*; John Wiley & Sons, Inc., **2014**; 231–240.

[60] a) Kundu, S.; Choi, J.; Wang, D. Y.; Choliy, Y.; Emge, T. J.; Krogh-Jespersen, K.; Goldman, A. S. Cleavage of Ether, Ester, and Tosylate $C(sp^3)$–O Bonds by an Iridium Complex, Initiated by Oxidative Addition of C–H Bonds. Experimental and Computational Studies. *J. Am. Chem. Soc.* **2013**, *135*, 5127–5143.

[61] In *Purification of Laboratory Chemicals (Sixth Edition)*; Armarego, W. L. F., Chai, C. L. L., Eds.; Butterworth-Heinemann: Oxford, **2009**.

[62] Herde, J. L.; Lambert, J. C.; Senoff, C. V; Cushing, M. A. Cyclooctene and 1,5-Cyclooctadiene Complexes of Iridium(I). In *Inorganic Syntheses, Volume 15*; John Wiley & Sons, Inc., **1974**, pp 18–20.

[63] Giordano, G.; Crabtree, R. H.; Heintz, R. M.; Forster, D.; Morris, D. E. Di-μ-Chloro-Bis(η^4-1,5-Cyclooctadiene) Dirhodium(I). In *Inorganic Syntheses, Volume 19*; John Wiley & Sons, Inc., **1979**, pp 218–220.

[64] Usón, R.; Oro, L. A.; Cabeza, J. A.; Bryndza, H. E.; Stepro, M. P. Dinuclear Methoxy, Cyclooctadiene, and Barrelene Complexes of Rhodium(I) and Iridium(I). In *Inorganic Syntheses, Volume 23*; John Wiley & Sons, Inc., **1985**; pp 126–130.

[65] Abel, E. W.; Bennett, M. A.; Wilkinson, G. 646. Norbornadiene-metal complexes and some related compounds. *J. Chem. Soc.* **1959**, 3178-3182.

[66] White, C.; Yates, A.; Maitlis, P. M.; Heinekey, D. M. (η^5-Pentamethylcyclopentadienyl)Rhodium and -Iridium Com-

pounds. In *Inorganic Syntheses, Volume 29*; John Wiley & Sons, Inc., **1992**; pp 228–234.

[67] Cross-peaks were integrated and processed with the EXSYCalc software distributed by Mestrelab research (http://www.mestrec.com).

[68] Frisch, M. J.; Trucks, G. W.; Schlegel, H. B.; Scuseria, G. E.; Robb, M. A.; Cheeseman, J. R.; Scalmani, G.; Barone, V.; Mennucci, B.; Petersson, G. A.; Nakatsuji, H.; Caricato, M.; Li, X.; Hratchian H. P. *et al.*, Gaussian, Inc.: Wallingford, CT, USA, **2009**.

[69] Lee, C.; Yang, W.; Parr, R. G. Development of the Colle-Salvetti correlation-energy formula into a functional of the electron density. *Phys. Rev. B* **1988**, *37*, 785–789.

[70] Becke, A. D. Density-functional thermochemistry. III. The role of exact exchange. *J. Chem. Phys.* **1993**, *98*, 5648–5652.

[71] Becke, A. D. A new mixing of Hartree–Fock and local density functional theories. *J. Chem. Phys.* **1993**, *98*, 1372–1377.

[72] Grimme, S.; Antony, J.; Ehrlich, S.; Krieg, H. A consistent and accurate ab initio parametrization of density functional dispersion correction (DFT-D) for the 94 elements H-Pu. *J. Chem. Phys.* **2010**, *132*, 154104.

[73] Tomasi, J.; Mennucci, B.; Cammi, R. Quantum Mechanical Continuum Solvation Models. *Chem. Rev.* **2005**, *105*, 2999–3094.

[74] Ehlers, A. W.; Böhme, M.; Dapprich, S.; Gobbi, A.; Höllwarth, A.; Jonas, V.; Köhler, K. F.; Stegmann, R.; Veldkamp, A.; Frenking, G. A set of f-polarization functions for pseudo-potential basis sets of the transition metals Sc-Cu, Y-Ag and La-Au. *Chem. Phys. Lett.* **1993**, *208*, 111–114.

[75] SAINT-PLUS: Area-Detector Integration Software, version 6.01; Bruker AXS: Madison, WI, 2001.

[76] SADABS program; University of Göttingen: Göttingen, Germany, 1999.

[77] Sheldrick, G. M. A short history of SHELX. *Acta Crystallogr., Sect. A: Fundam. Crystallogr.* **2008**, *64*, 112–122.

[78] Sheldrick, G. M. Crystal structure refinement with SHELXL. *Acta Crystallogr., Sect. C: Cryst. Struct. Commun.* **2015**, *71*, 3–8.

[79] Farrugia, L. J. WinGX and ORTEP for Windows: an update. *J. Appl. Crystallogr.* **2012**, *45*, 849–854.

[80] Nardelli, M. PARST95 - an update to PARST: a system of Fortran routines for calculating molecular structure parameters from the results of crystal structure analyses. *J. Appl. Cryst.* **1995**, *28*, 659.
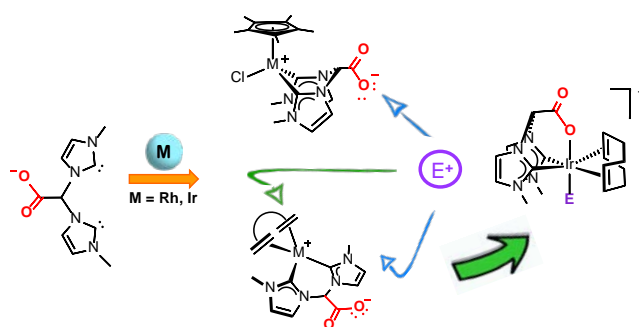
Table of Contents artwork

A series of water-soluble zwitterionic rhodium and iridium complexes featuring a carboxylate bridge-functionalized bis-N-heterocyclic carbene ligands have been synthesized. The uncoordinated carboxylate fragment is reactive towards electrophiles affording cationic complexes featuring carboxy- and methoxycarbonyl functionalized ligands. In contrast, the oxidation of the iridium center results in iridium(III) octahedral complexes stabilized by the tripodal coordination mode of the functionalized bis-NHC ligand.